

Geotechnical Assessment of Tailings Facilities Cantung Mine, Northwest Territories



PRESENTED TO

**North American Tungsten Corp., c/o Alvarez and Marsal Canada Inc. and
Crown-Indigenous Relations and Northern Affairs Canada**

MARCH 15, 2021

ISSUED FOR USE

FILE: 704-ENW.WENW03039-05

This page intentionally left blank.

EXECUTIVE SUMMARY

Introduction

Tetra Tech Canada Inc. (Tetra Tech) was retained by Alvarez & Marsal Canada Inc. (A&M), in its capacity as court-appointed monitor of North American Tungsten Corporation Ltd. (NATCL), to conduct a geotechnical assessment of the existing tailings ponds at the Cantung Mine, NT. The geotechnical assessment comprises part of an overall site assessment aimed at developing concept level remedial options for site closure. This report pertains solely to the existing pond condition. Concept remediation designs will be presented in the remedial option assessment.

The primary issue related to tailings dam performance is the potential liquefaction (seismic liquefaction) of foundation soils underlying the tailings dam structures during an earthquake event. Seismic liquefaction refers to the rapid reduction of shear strength of a soil during ground motion resulting in potential settlement and lateral movement of the overlying dam structures; this movement, if excessive, could lead to failure of the dam structure. This represents a long-term stability risk and requires geotechnical evaluation and design.

The primary purposes of the geotechnical evaluation are to:

- Assess the geotechnical stability of the existing tailings ponds, based on updated geotechnical data; and
- Provide guidance for remedial option development.

The geotechnical evaluation was completed based on guidelines published by the Canadian Dam Association (CDA). These guidelines are accepted by industry and regulators as a minimum for the design and evaluation of dam structures. Deviations from these guidelines are permitted under specific circumstances; however, recommended CDA guidelines were carried forward for concept level analysis as part of this study.

Project Details

The Cantung Mine site is located in the Northwest Territories (NT), approximately 300 km north of Watson Lake, Yukon, and just east of the Yukon-NT border. Road access to the mine site is possible from Watson Lake, via Highway 4 (Robert Campbell Highway) and then along Highway 10 (Nahanni Range Road). Most of the mine infrastructure is located on the west side of the Flat River valley and is constructed on benches at various elevations. The Flat River runs along the valley floor in a roughly northwest-southeast direction.

Cantung Mine is a past-producing, open pit and underground tungsten mine that operated intermittently from the early 1960s to 2015. The mine ceased operations in late 2015 and is presently in care and maintenance.

The site contains typical mining infrastructure including mill and surface plant facilities, water management facilities, an open pit, underground mine workings, waste rock storage areas, ore stockpiles, tailings ponds, landfills, and various site access roads. There is also a townsite that contains structures such as single family homes, apartment complexes, and a recreational facility. Most of these structures are in poor physical condition and are not in regular use today.

The Cantung Mine has five tailings storage facilities (historically referred to as Tailings Ponds (TP) 1 through 5) which are located adjacent to the Flat River. The facilities comprise granular dam structures with impounded tailings. The tailings have drained with time, and there is limited or no ponding on the surface. For the purposes of this report the existing tailings storage facilities retain the term “tailings ponds”, consistent with past practice. Further description of the tailings ponds is provided in Table 1.

Table 1: Summary of Tailings Pond Facilities

Name	Active Period	Stored Tailings Volume (m ³)	Current Cover Condition
TP1	1965 to early 1970s	263,000 (combined with TP2)	Covered with 1.0 to 3.0 m of fill consisting of a mix of granular material and tailings
TP2	1965 to early 1970s	263,000 (combined with TP1)	Covered with 1.0 to 3.0 m of fill consisting of a mix of granular material and tailings
TP3	1971 to 2007	1,316,000	Uncovered
TP4	1971 to 2007 (exfiltration pond*) 2007 to 2015 (tailings pond)	850,000	Uncovered
TP5	2007 (exfiltration pond) 2013 to 2015 (tailings pond)	587,000	Uncovered

*exfiltration pond – engineered structure to contain solids while allowing mine water to gradually drain/filter through.

Geotechnical Site Data

Multiple geotechnical site investigations have been completed since the mid 1970s to evaluate foundation soils, groundwater conditions, dam composition, borrow sources, and tailings properties. These investigations have been completed within and around the existing tailings pond footprints and at potential new tailings storage locations.

In total, 17 investigations have been completed since 1976. Drilling methods have included Becker hammer (instrumented and non-instrumented), air rotary, ODEX tricone, mechanical excavation, and sonic drilling. Cone penetration testing (CPT) was completed concurrently with several investigations, providing continuous material properties (strength and moisture content) through the soil profile. Standard penetration testing (SPT), Becker penetration testing, and large penetration testing also provided soil strength information at discrete locations throughout the soil profile.

The most recent investigation was completed by Tetra Tech in 2019 to characterize foundation soils and fill in gaps or uncertainties identified in previous investigation results. The main focus was on characterizing the liquefaction potential of foundation soils underlying the existing tailings dams, although stratigraphic information was collected at some locations. Two drilling methods were used: instrumented Becker Penetration Testing (iBPT) and sonic drilling. A total of 33 iBPT and 16 sonic boreholes were drilled in the five tailings ponds (TP1 to TP5).

Terrain assessments have also been completed for the Cantung Mine site to describe the surficial geology and associated deposition history. As part of the geotechnical work, Tetra Tech reviewed and updated the existing site terrain mapping. This included a review of available geotechnical investigation reports and a field program to refine soil textures and ground truth the terrain assessment.

Site Model

Methodology

Tetra Tech developed a geotechnical model of the tailings ponds (foundation conditions and superstructure) by integrating data from the geotechnical investigations, historical air photos, pre-development terrain mapping, and design and construction record reports. Interpretation of the data was often required when comparing multiple sources as a better understanding of the local stratigraphy and depositional history was formed. This model assisted in evaluating the overall performance of the tailings ponds.

A site-specific seismic hazard assessment was completed to determine the design earthquake loading specific to the Cantung Mine site. The target earthquake hazard level was assessed in accordance with the CDA guidelines for the passive closure phase at an annual exceedance probability (AEP) of 1 in 2,475 years. The analysis determined a design earthquake magnitude for the site of M6.54 and a peak ground acceleration (PGA) of 0.210g.

The liquefaction potential of the tailings dams and foundation soils was evaluated based on the site model, geotechnical investigation results, and the seismic hazard assessment. The liquefaction triggering assessment was undertaken following the approach outlined by Boulanger and Idriss (2014). Preliminary assessment of the liquefaction potential of the impounded tailings was also completed; however, the primary focus of the analyses was on the granular fill of the dams and underlying foundation material.

Liquefaction potential in the foundation soils was evaluated for earthquake events only. Static liquefaction, associated with material placement, and increasing porewater pressure, is not an issue at the Cantung Mine since the tailings ponds are largely drained and no future loading associated with tailings deposition or dam construction is expected.

Model Summary

The tailings ponds are generally located on glaciofluvial and fluvial valley infill, with some colluvium sourced from the valley side slopes. Bedrock under the dam structures is deep (>30 m) and groundwater is typically below the original ground elevation and base of the tailings ponds, typically following the original ground contours.

The mine site is situated in an area of extensive discontinuous permafrost, which is defined as regions with approximately 50% to 90% of land underlain by permafrost (Natural Resources Canada 1995). Previous investigations have identified some pockets of permafrost at the site; however, these are generally isolated areas and the site can largely be assumed to be underlain by unfrozen ground conditions.

Geotechnical investigations and analyses have identified liquefiable soils under TP1 through TP4, which are generally located on glaciofluvial and colluvium material. The liquefiable soils extend under the crest and downstream toe of TP1 and TP2, but are generally limited to the downstream toe area of TP3. Liquefiable soils were identified under the downstream toe of TP4 and were present, to a limited extent, at mid-slope as well. The softening of foundation soils following a seismic event can be expected under TP5; however, actual liquefaction of the foundation soil is not anticipated.

The tailings themselves show a varying response to seismic loading. In the upper portion of the tailings ponds, the tailings are largely unsaturated and are generally not susceptible to liquefaction during seismic loading. Moisture contents increase toward the base of the deposits, nearing saturated conditions at depth. Analysis shows a potential for basal tailings liquefaction in TP1 and TP2, and some degree of softening in TP3 and TP4; however, the dam embankments are not susceptible to liquefaction.

The containment dams are constructed of local glaciofluvial and fluvial materials consisting of a mixture of silts, sands, and gravels, with occasional cobbles and boulders. As-built records show they were constructed in stages using upstream, downstream, and centerline methods, to provide tailings containment capacity. Tailings have typically been deposited subaerially around the pond perimeter resulting in segregated beach deposits. Limited segregated tailing placement (from cyclone processing) also occurred during underground backfill operations.

The Cantung tailings dams are currently classified as having a Significant consequence of failure based on CDA guidelines and have been analyzed accordingly. CDA guidelines allow dams in closure to be declassified to waste structures, provided it can be proven the tailings pond contents will not liquefy during seismic loading. Current analysis suggests the potential for tailings liquefaction at the base of the pond and further study is required to determine if the dams can be classified as waste structures. For the purposes of this report, the tailings dams were treated as dam structures, per CDA guidelines.

Geotechnical Analysis

Geotechnical analyses were completed on the existing dam structures. This included limit equilibrium stability analyses and two-dimensional deformation analysis.

Stability Analyses

Limit equilibrium analyses were conducted to determine the factor of safety against slope failure (FS_{slope}) of the existing tailings facilities on site. Factors of safety represent a measure of slope stability and are defined as the ratio of those forces resisting slope movement to those forces causing movement. They provide a level of conservatism to account for model inaccuracies, knowledge of stratigraphy, and uncertainties in soil parameters. A FS_{slope} less than 1 indicates a potential for slope instability, whereas a FS_{slope} greater than 1 is less susceptible to slope instability.

The principles underlying the method of limit equilibrium for slope stability analyses are as follows:

- A slip mechanism is postulated;
- The shear stresses required to equilibrate the assumed slip mechanism is calculated statically;
- The factor of safety is defined as the ratio of the available shear strength to the calculated shear stresses required for equilibrium; and
- The slip surface with the lowest factor of safety is determined through iteration.

The long-term slope stability of the tailing ponds was evaluated under three design scenarios:

- Static loading: Geotechnical stability loading condition that considers the existing slope condition without ground acceleration due to an earthquake;
- Seismic (pseudo-static) loading: Stability loading condition that considers forces generated during an earthquake event; and
- Post-seismic loading: Stability loading condition that considers modified strength parameters resulting from earthquake activity (static loading with residual undrained shear strength ratios assigned to the materials predicted to experience a reduction in strength).

Stability analyses were completed on representative cross-sections from TP1 through TP4. TP5 is located upgradient of the other dams. Analysis and previous studies indicate TP5 is located on non-liquefiable foundation material. As such, TP5 is not considered a critical structure and was not included in more detailed analyses.

Material properties, such as density, friction angle, cohesion, and liquefied residual strength ratio, were selected based on investigation data, correlations with in situ data, published relationships, and engineering judgement. Zones of potential liquefaction were estimated from the Boulanger and Idriss (2014) approach noted above.

Calculated FS_{slope} values are summarized as follows:

- Static stability analyses for deep seated failures typically meet or are slightly below the minimum CDA FS_{slope} of 1.5, with values ranging from 1.4 to 1.9.
- FS_{slope} for static shallow failures on the downstream dam slopes ranged from 1.0 to 1.6. Shallow failures typically comprise sloughing or slumping of localized areas of the downstream slope in response to precipitation events or steep slope geometry. They do not pose a threat to the integrity of the dam; however, maintenance may be required following seismic events or the slopes may need to be flattened to improve the FS_{slope} .
- FS_{slope} for the pseudo-static loading condition (during ground shaking) ranged from 1.0 to 1.1 for deep rotational failures (through the foundation soils), meeting the minimum CDA criteria of 1.0.
- FS_{slope} for pseudo-static shallow failures were less than 1.0; however, as noted above, these do not represent critical failures and could be addressed through maintenance or slope flattening.
- Under post-seismic conditions, FS_{slope} for all sections fall below recommended minimum CDA guidelines of 1.2 to 1.3. FS_{slope} for deep seated rotational failures range from 0.5 to 1.1, and FS_{slope} for translational (sliding) failures range from 0.1 to 1.1.

In summary, factors of safety (FS_{slope}) for static and pseudo-static loading conditions for TP1 through TP4 generally meet CDA guidelines; however, instability is observed in the post-seismic condition as a result of the liquefiable foundation soils underlying the dams.

Stability analysis results indicate the tailings dams are stable (except for localized, small scale deformations) under existing conditions and during ground shaking; however, liquefaction of foundation soils following the design earthquake event reduces foundation soils strengths to the point where potential instability may occur.

Deformation Analysis

Non-linear effective stress analyses were completed using the computer program FLAC Version 8.0 to estimate the extent of seismic liquefaction and deformation of the tailings ponds. The stress analyses provided a more robust estimate of liquefaction development under the tailings dams, as well as an estimate of settlement and lateral shifting following an earthquake event. This offers additional context surrounding the impacts of a potential dam failure. Whereas, the stability analysis indicates there is a problem, the FLAC analysis helps define the extent and magnitude of a potential failure.

The FLAC analyses generally indicate less liquefaction development under the dams than the simplified method based on Boulanger and Idriss (2014). This suggests there is some conservatism in the stability analyses since the stability analysis incorporated the liquefiable layers predicted with the simplified method. However, this is considered acceptable for a concept level study.

Sensitivity analyses were conducted to evaluate the predicted liquefaction extents and associated displacements for a range of geotechnical parameters. These parameters comprised $(N_1)_{60-cs}$ (penetration resistance), V_{s1} (initial soil stiffness), and k (hydraulic conductivity). The sensitivity analyses also considered increases in groundwater elevations upstream of the dam. An additional analysis was conducted by developing a pessimistic soil profile for comparison with the baseline case. A reduction in $(N_1)_{60-cs}$ had the largest impact on the horizontal displacements

over the range of parameters examined. In general, the deformations were reasonably unaffected for the other parameters.

Deformation analyses show predicted deformations (lateral and vertical) are less than 1 m following the design earthquake event. This suggests the risk of a breach style failure, where tailings would discharge to the Flat River, is relatively low. This is a function of estimated maximum deflections in the order of 1 m coupled with unsaturated tailings (in the upper tailings pond) that would be unlikely to liquefy during the design seismic event. There is a potential risk that surface flow could initiate erosion and transport of the tailings; however, this can be mitigated with the placement of appropriate cover material.

Discussion

Overall, the dams are considered to be stable under static loading conditions, with the exception of potential shallow downstream slumping or sloughing. Seismic events would initiate slope deformation and movement; however, the risk of massive slope failure and tailings run out is considered low.

Addressing the potential instability observed during post-seismic loading can be broadly approached by either maintaining the existing condition, implementing in situ engineering measures, or removing material overlying potentially liquefiable soils. Possible options under consideration are summarized below and further developed in the ROA.

- **Maintain existing geotechnical condition:** The existing tailings dam slope geometry could be maintained and monitored for acceptable performance. This approach would require a risk assessment that considers the likelihood and consequence of a breaching type failure.
- **Ground improvement:** Ground improvement techniques such as stone columns or jet grouting could be used to provide additional stability at the dam toe during an earthquake event.
- **Downstream stabilization buttress:** A downstream buttress could be constructed to improve post-seismic stability and reduce deformations.
- **Complete tailings excavation:** Tailings and the containment dam could be excavated in their entirety. Tailings could be dry stacked at a facility with foundation soils not susceptible to post-seismic liquefaction. Dam material could then be used as borrow material for site reclamation activities.
- **Partial tailings excavation:** This option is similar to the complete tailings excavation except that excavation would be limited to the area underlain by, and close to, liquefiable soils.

TABLE OF CONTENTS

EXECUTIVE SUMMARY	I
1.0 INTRODUCTION.....	1
2.0 BACKGROUND INFORMATION	1
2.1 General	1
2.2 Project Description.....	2
2.3 Geotechnical Investigations.....	3
2.3.1 Geotechnical Investigations.....	3
2.3.2 Laboratory Testing Results.....	5
2.4 Survey Coordinate System	5
3.0 TAILINGS POND DEVELOPMENT.....	5
3.1 General	5
3.2 Tailings Ponds 1 and 2	6
3.3 Tailings Pond 3	8
3.4 Tailings Pond 4	9
3.5 Tailings Pond 5	11
4.0 SUBSURFACE CONDITIONS	12
4.1 Surficial Geology.....	12
4.1.1 Depositional History.....	12
4.1.2 Soil Types and Occurrences.....	12
4.2 Groundwater	13
4.3 Permafrost Conditions	14
5.0 GEOLOGICAL MODEL.....	14
5.1 Model Development.....	14
5.2 Interpreted Conditions	15
5.2.1 Tailings Ponds 1 and 2	15
5.2.2 Tailings Ponds 3, 4, and 5	16
6.0 DESIGN GUIDELINES.....	16
6.1 Dam Classification	16
6.2 Review of Design Guidelines for Tailings Dams.....	17
6.2.1 CDA Guidelines	17
6.2.2 Basis of Evaluation	19
6.2.3 Declassification	19
7.0 SITE-SPECIFIC SEISMIC HAZARD ASSESSMENT	19
8.0 LIQUEFACTION ASSESSMENTS.....	20
8.1 Methodology	21
8.1.1 Site Response Analysis	21
8.1.2 Liquefaction Potential	21

8.2	Liquefaction Assessment Results	22
8.2.1	Tailings Ponds 1 and 2	22
8.2.2	Tailings Pond 3	23
8.2.3	Tailings Pond 4	23
8.2.4	Tailings Pond 5	23
8.2.5	Tailings Storage Facility 6.....	23
8.3	Tailings Liquefaction Potential	24
8.3.1	Tailings Saturation Estimate	24
8.3.2	Results	25
9.0	SLOPE STABILITY ANALYSES.....	25
9.1	Methodology and Design Criteria	25
9.1.1	SLOPE/W Software	25
9.1.2	Design Criteria for Factor of Safety against Slope Failure	26
9.2	Stability Analysis Cases and Input Data	26
9.2.1	Stability Cases Evaluated	26
9.2.2	Sections Evaluated	27
9.2.3	Material Properties.....	27
9.2.4	Interpreted Liquefiable Layers	28
9.2.5	Sensitivity Analyses	28
9.3	Stability Analysis Results	29
10.0	DEFORMATION ANALYSES.....	31
10.1	Methodology	32
10.1.1	FLAC Software	32
10.1.2	Geotechnical Parameters and Constitutive Models	32
10.1.3	Input Ground Motions	33
10.1.4	Model Configuration and Boundary Conditions	34
10.1.5	Output 34	
10.2	TP4 – Section D-D'	35
10.2.1	Section D-D' Input Parameters	35
10.2.2	Section D-D' Baseline Analyses	35
10.2.3	Section D-D' Sensitivity Analyses.....	37
10.2.4	Section D-D' Discussion	38
10.3	TP1 – Section A-A'	39
10.3.1	Section A-A' Input Parameters	39
10.3.2	Section A-A' Baseline Analyses.....	40
10.3.3	Section A-A' Sensitivity Analyses	40
10.3.4	Section A-A' Discussion.....	42
11.0	SUMMARY.....	42
12.0	CLOSURE.....	46
	REFERENCES	47

LIST OF TABLES IN TEXT

Table 1: Summary of Tailings Pond Facilities	ii
Table 2-1: Summary of Tailings Pond Facilities	2
Table 2-2: Historical Investigations	3
Table 3-1: Tailings Pond 1 and 2 Construction Sequencing.....	7
Table 3-2: Tailings Pond 3 Construction Sequencing.....	9
Table 3-3: Tailings Pond 4 Construction Sequencing.....	10
Table 3-4: Tailings Pond 5 Construction Sequencing.....	11
Table 6-1: Summary of Dam Classification of Existing Tailings Facilities (after SRK 2017b).....	17
Table 6-2: CDA Recommended Earthquake Loadings (from Table 4-2: Target Levels for Earthquake Hazards, Standards-Based Assessments for Closure – Passive Care Phase)	18
Table 6-3: CDA Recommended Target Factors of Safety for Operation, Transition, and Closure Phases (from Tables 3-4 and 3-5, CDA Technical Bulletin, 2014)	18
Table 7-1: Selected Ground Motion Time Histories	20
Table 9-1: Factors of Safety Considered in Slope Stability Analyses	26
Table 9-2: Geotechnical Input Parameters in Slope/W Analyses	28
Table 9-3: Summary of Minimum Calculated Factors of Safety for Static and Seismic Scenarios	30
Table 9-4: Summary of Minimum Calculated Factors of Safety for Post-Seismic Scenario	31
Table 10-1: Calculated Cumulative Absolute Velocities (CAV) for each Earthquake Record.....	33
Table 10-2: Key Geotechnical Input Parameters for Section D-D' Baseline Analyses	35
Table 10-3: Post-Seismic Displacements – Section D-D' Baseline Analyses (Maximum-Intensity Earthquake Record)	36
Table 10-4: Post-Seismic Displacements – Section D-D' Baseline Analyses (Average of 11 Earthquake Records).....	36
Table 10-5: Section D-D' Sensitivity Analysis Cases.....	37
Table 10-6: Post-Seismic Displacements – Section D-D' Pessimistic vs. Baseline Analyses (Maximum-Intensity Earthquake Record)	38
Table 10-7: Key Geotechnical Input Parameters for Section A-A' Baseline Analyses	39
Table 10-8: Post-Seismic Displacements – Section A-A' Baseline Analyses (Maximum-Intensity Earthquake Record)	40
Table 10-9: Post-Seismic Displacements – Section A-A' Baseline Analyses (Average of 11 Earthquake Records).....	40
Table 10-10: Section A-A' Sensitivity Analysis Cases	41
Table 10-11: Post-Seismic Displacements – Section A-A' Pessimistic vs. Baseline Analyses (Maximum-Intensity Earthquake Record)	42

APPENDIX SECTIONS

TABLES

Table A	Detailed Historical Geotechnical Investigations in Tailings Pond Footprints
Table B	Compiled Borehole Details
Table C	Compiled Instrumentation Data
Table D	Historical Slope Stability Analyses – Summary of Material Properties

FIGURES

Figure 2-1	Location of Cantung Mine
Figure 2-2	General Site Plan
Figure 2-3	Mine Site and Townsite Overview
Figure 2-4	Tailings Ponds 1 and 2 – Borehole Location Plan
Figure 2-5	Tailings Ponds 3 and 4 – Borehole Location Plan
Figure 2-6	Tailings Pond 5 – Borehole Location Plan
Figure 2-7	Proposed Tailings Storage Facility 6 Area – Borehole Location Plan
Figure 3.1-1	Tailings Pond 1 and 2, 1960 Plan View
Figure 3.1-2	Tailings Pond 1 and 2, 1968 Plan View
Figure 3.1-3	Tailings Pond 1 and 2, 1971 Plan View
Figure 3.1-4	Tailings Pond 1 and 2, 1976 Plan View
Figure 3.1-5	Tailings Pond 3,4 and 5, 1960 Plan View
Figure 3.1-6	Tailings Pond 3,4 and 5, 1968 Plan View
Figure 3.1-7	Tailings Pond 3,4 and 5, 1971 Plan View
Figure 3.1-8	Tailings Pond 3,4 and 5, May 1974 Plan View
Figure 3.1-9	Tailings Pond 3,4 and 5, 1976 Plan View
Figure 3.1-10	Tailings Pond 3,4 and 5, 1982 Plan View
Figure 3.1-11	Tailings Pond 3,4 and 5, 2002 Plan View
Figure 3.1-12	Tailings Pond 3,4 and 5, 2007 Plan View
Figure 3.1-13	Tailings Pond 3,4 and 5, 2009 Plan View
Figure 3.1-14	Tailings Pond 3,4 and 5, 2012 Plan View
Figure 3.2-1	Tailings Pond 1 and 2, Typical Cross-section
Figure 3.2-2	Tailings Pond 3, Typical Cross-section
Figure 3.2-3	Tailings Pond 4, Typical Cross-section
Figure 4-1	Pre-Development Terrain Map
Figure 4-2	Interpreted Groundwater Contours
Figure 4-3a	Tailings Pond 1 and 2 – Instrumentation Plan
Figure 4-3b	Tailings Pond 3 and 4 – Instrumentation Plan
Figure 5-1	Tailings Pond Geological Model – Section A-A
Figure 5-2	Tailings Pond Geological Model – Section B-B
Figure 5-3	Tailings Pond Geological Model – Section K-K
Figure 5-4	Tailings Pond Geological Model – Section C-C
Figure 5-5	Tailings Pond Geological Model – Section D-D
Figure 5-6	Tailings Pond Geological Model – Section E-E
Figure 5-7	Tailings Pond Geological Model – Section F-F
Figure 5-8	Tailings Pond Geological Model – Section G-G
Figure 5-9	Tailings Pond Geological Model – Section H-H
Figure 5-10	Tailings Pond Geological Model – Section I-I
Figure 5-11	Tailings Pond Geological Model – Section J-J

APPENDICES

Appendix A	Tetra Tech's Limitations on Use of this Document
Appendix B	Site-Specific Seismic Hazard Assessment for Cantung Project
Appendix C	Liquefaction Potential Assessment Results
Appendix D	Stability Analysis Figures
Appendix E	Deformation Analysis Figures

ACRONYMS, ABBREVIATIONS, AND GLOSSARY OF KEY TERMS

Acronyms/Abbreviations	Definition
AEP	Annual Exceedance Probability
A&M	Alvarez & Marsal Canada Inc.
BGC	BGC Engineering Inc.
BPT	Becker Penetration Test
CDA	Canadian Dam Association
CRR	Cyclic Resistance Ratio
CSR	Cyclic Stress Ratio
CU	Consolidated Undrained
DCPT	Dynamic Cone Penetration Test
DST	Downhole Seismic Test
EBA	EBA Engineering Consultants Ltd.
EP	Exfiltration Pond
ESA	Environmental Site Assessment
FLAC	Fast Lagrangian Analysis of Continua – Finite difference computer software used to evaluate liquefaction and ground deformation by numerical modelling
FS _{liq}	Factor of Safety against Liquefaction
FS _{slope}	Factor of Safety against Slope Failure
Golder	Golder Associates Ltd.
GSC	Geological Survey of Canada
iBPT	Instrumented Becker Penetration Test
Knight Piesold	Knight Piesold Consulting Ltd.
LPT	Large Penetration Test
M _w	Mean Moment Magnitude
NATCL	North American Tungsten Corporation Ltd.
NBCC	National Building Code of Canada
OSC	Onur Seemann Consulting Inc.
PDA	Pile Driving Analyzer
PGA	Peak Ground Acceleration
Post-Seismic	Stability loading condition that considers modified strength parameters resulting from earthquake activity
PSHA	Probabilistic Seismic Hazard Assessment
Pseudo-Static	Stability loading condition that considers forces generated during an earthquake event

Acronyms/Abbreviations	Definition
SCPT	Seismic Cone Penetration Test
Shear Strength	Soil mechanics term used to describe the internal strength of a soil mass that provides resistance to shear failure
SPT	Standard Penetration Test
SRK	SRK Consulting (Canada) Inc.
Static	Stability loading condition that considers the existing slope condition without ground acceleration due to an earthquake
TCAMP	Tailings Containment Area Monitoring Plan
Tetra Tech	Tetra Tech Canada Inc.
Tetra Tech EBA	Tetra Tech EBA Inc.
TP	Tailings Pond
TSF	Tailings Storage Facility
UTM	Universal Transverse Mercator
Vs	Shear Wave Velocity

LIMITATIONS OF REPORT

This report and its contents are intended for the sole use of North American Tungsten Corporation Ltd. c/o Alvarez & Marsal Canada Inc. and their agents. Tetra Tech Canada Inc. (Tetra Tech) does not accept any responsibility for the accuracy of any of the data, the analysis, or the recommendations contained or referenced in the report when the report is used or relied upon by any Party other than North American Tungsten Corporation Ltd. c/o Alvarez & Marsal Canada Inc., or for any Project other than the proposed development at the subject site. Any such unauthorized use of this report is at the sole risk of the user. Use of this document is subject to the Limitations on Use of this Document attached in the Appendix or Contractual Terms and Conditions executed by both parties.

1.0 INTRODUCTION

Tetra Tech Canada Inc. (Tetra Tech) was retained by Alvarez & Marsal Canada Inc. (A&M), in its capacity as court-appointed monitor of North American Tungsten Corporation Ltd. (NATCL), to conduct a geotechnical assessment of the tailings ponds located at Cantung Mine, NT.

The purpose of the evaluation is to assess the geotechnical stability of the existing tailings facilities (referred to as “tailings ponds” in this report, consistent with past practice) and provide guidance for subsequent remedial option development. The evaluation builds on previous analyses and incorporates site data from the recent 2019 investigation program.

Work completed as part of the assessment includes the following:

- Data Compilation and Review (Sections 2.0 through 5.0)
 - Review and evaluate data from historical geotechnical investigations, dam safety reviews, and other available sources (e.g., geologic reports, air photographs, borehole logs, field tests, and laboratory tests);
 - Evaluate recent investigation data (Tetra Tech 2019a) to update previously developed site models and analyses; and
 - Develop a pre-development terrain map and geological model from available geotechnical data.
- Data Analysis (Sections 6.0 through 10.0)
 - Review design guidelines relating to tailings dams and select appropriate target factors of safety for the geotechnical analyses;
 - Complete a site-specific seismic hazard assessment to characterize the seismic activity at the mine location;
 - Evaluate liquefaction potential at several critical locations to determine the extent of potentially liquefiable materials underlying the tailings ponds;
 - Analyze tailings pond stability using limit equilibrium analysis (stability analysis) for static, pseudo-static, and post-seismic cases; and
 - Evaluate liquefaction and ground deformation by numerical modelling using the finite difference computer software Fast Lagrangian Analysis of Continua (FLAC).
- Discussion and Recommendations (Section 11.0)
 - Assess results and provide preliminary recommendations for potential remediation options.

2.0 BACKGROUND INFORMATION

2.1 General

The Cantung Mine site is located in the Northwest Territories (NT), approximately 300 km north of Watson Lake, Yukon, and just east of the Yukon-NT border (Figure 2-1). The approximate coordinates are latitude 60.969° N and

longitude 128.233° W, with Universal Transverse Mercator (UTM Zone 9) coordinates of 541,000 E and 6,871,000 N (NAD83).

Cantung Mine is a past-producing, open pit and underground tungsten mine that operated intermittently from the early 1960s to 2015. It was originally operated as an open pit mining operation but later moved to underground mining in the early 1970s. The mine is currently under care and maintenance. Road access to the mine site is possible from Watson Lake, via Highway 4 (Robert Campbell Highway) and then along Highway 10 (Nahanni Range Road) for a total distance of 300 km. NATCL maintains the final 65 km of the access road from the mine site to km 134 on the Nahanni Range Road. The Yukon government is responsible for maintaining the remainder of the road from km 134 to Watson Lake (NATCL 2014).

Figure 2-2 presents a general site plan, showing the locations of the primary mining facilities and site infrastructure. It also highlights the proximity of the mine's infrastructure to the Flat River. The mine site and townsite layout around the mill and accommodation areas are shown on Figure 2-3. Additional details pertaining to site infrastructure and mining facilities are presented in the Conceptual Site Model (CSM; Tetra Tech 2020b) and Phase III Environmental Site Assessment (ESA; Tetra Tech 2020a) developed for the site.

2.2 Project Description

NATCL sought creditor protection in 2015 and A&M was appointed as the monitor of the Cantung Mine site. The mine ceased operations in late 2015 and is presently under care and maintenance.

The Cantung Mine has five tailings pond facilities (TP1 to TP5) which are shown on Figure 2-3. TP1 and TP2 are located immediately northeast and below the mill site while TP3, TP4, and TP5 are located southeast of the townsite. A summary of the tailings ponds uses and current conditions are provided in Table 2-1. All the tailings pond containment dams are constructed of local glaciofluvial and fluvial materials consisting of a mixture of silts, sands, and gravels, with occasional cobbles and boulders. They have been constructed in stages as required to provide tailings containment capacity.

Table 2-1: Summary of Tailings Pond Facilities

Name	Active Period	Current Condition
TP1	1965 to early 1970s	<ul style="list-style-type: none"> Covered with 1.0 m to 3.0 m of fill Two storage structures on TP1 surface: metal clad storage building (381 m²), steel Quonset (232 m²) Storage area for site materials and equipment
TP2	1965 to early 1970s	<ul style="list-style-type: none"> Covered with 1.0 m to 3.0 m fill Storage area for site materials and equipment Approximate combined surface area (with TP1) of 4.2 ha Approximate combined tailings volume (with TP1) of 263,000 m³
TP3	1971 to 2007	<ul style="list-style-type: none"> Uncovered Approximate tailings volume of 1,316,000 m³
TP4	1971 to 2007 (exfiltration pond) 2007 to 2015 (tailings pond)	<ul style="list-style-type: none"> Uncovered Approximate combined surface area (with TP3) of 14.6 ha Approximate tailings volume of 850,000 m³
TP5	2007 (exfiltration pond) 2013 to 2015 (tailings pond)	<ul style="list-style-type: none"> Uncovered Approximate surface area of 3.0 ha Approximate tailings volume of 587,000 m³

Prior to operations ceasing in 2015, a dry stacked tailings storage facility (referred to as proposed TSF6) was being investigated to provide additional storage capacity for mining operations. The facility was to be constructed approximately 4.5 km southeast of the mine site in an area commonly known as the old rifle range (Tetra Tech 2014b). This area is mostly undisturbed but contains access roads used for past geotechnical drilling investigations.

2.3 Geotechnical Investigations

2.3.1 Geotechnical Investigations

Several geotechnical investigations have been conducted within and around the tailings pond facilities over the mine's lifespan, as summarized in Table 2-2. The most recent program was completed by Tetra Tech in the summer of 2019 (Tetra Tech 2019a). This program provided a significant amount of data to evaluate the liquefaction potential under the tailings dams and helped to fill gaps in the soil stratigraphy data.

The investigation results supported the development of a pre-development terrain map, geological model, and design cross-sections (discussed in Section 5.0). Figures 2-4 to 2-7 show the locations of the historical boreholes as well as the locations of the cross-sections that were evaluated for each tailings pond.

Table 2-2: Historical Investigations

Company	Year	Investigation	Drilling Methodology	Available Data
Golder	1976	TP1 and TP5 Geotechnical Investigation	Becker Hammer (Open-ended)	<ul style="list-style-type: none"> Soil Stratigraphy Index Properties Strength Properties (Tailings)
Golder	1977	TP1 to TP4 Hydrology Investigation	Becker Hammer (Open-ended)	<ul style="list-style-type: none"> Soil Stratigraphy Index Properties
Golder	1982	TP1 to TP4 Hydrogeological Investigation	Air Rotary	<ul style="list-style-type: none"> Soil Stratigraphy Index Properties
EBA	2005	TP5 Geotechnical Investigation	Odex Tricone	<ul style="list-style-type: none"> Soil Stratigraphy SPT DCPT
EBA	2007	Ski Hill Borrow Site Testpit Investigation	Komatsu PC400 Excavator	<ul style="list-style-type: none"> Soil Stratigraphy Index Properties
EBA	2007	TP4 Geotechnical Investigation	Becker Hammer (Open and Closed-ended)	<ul style="list-style-type: none"> Soil Stratigraphy SPT BPT Index Properties
EBA	2007	TP4 Instrumentation Program	Air Rotary & Odex Tricone	<ul style="list-style-type: none"> Soil Stratigraphy
EBA	2009	Site Wide Groundwater Investigation	Odex Tricone	<ul style="list-style-type: none"> Soil Stratigraphy
Knight Piesold	2010	TP3 and TP4 Geotechnical Investigation	Sonic	<ul style="list-style-type: none"> Soil Stratigraphy SPT SCPT Index Properties Strength Properties

Table 2-2: Historical Investigations

Company	Year	Investigation	Drilling Methodology	Available Data
Knight Piesold	2011	TP3 and TP4 Geotechnical Investigation	Sonic	<ul style="list-style-type: none"> Soil Stratigraphy SPT SCPT Index Properties Strength Properties
EBA, A Tetra Tech Company	2011	TP1 and TP2 Geotechnical Investigation and Monitoring Well Installations	Sonic	<ul style="list-style-type: none"> Soil Stratigraphy SPT Index Properties
Knight Piesold	2012	EP1 ¹ Geotechnical Investigation	Sonic	<ul style="list-style-type: none"> Soil Stratigraphy SPT SCPT
EBA, A Tetra Tech Company	2012	EP1 ¹ and TP5 Geotechnical Investigation	Sonic	<ul style="list-style-type: none"> Soil Stratigraphy SPT SCPT Index Properties
EBA, A Tetra Tech Company	2012	Geotechnical Investigation for proposed TSF6	Sonic & Hitachi 270 Excavator	<ul style="list-style-type: none"> Soil Stratigraphy SPT SCPT DST Index Properties
EBA, A Tetra Tech Company	2013	Geotechnical Investigation for proposed TSF6, TSF7, and TSF4B	Sonic	<ul style="list-style-type: none"> Soil Stratigraphy LPT DST Index Properties
SRK	2016	TP1 to TP5 Geotechnical Investigation	Becker Hammer (Open and Closed-ended)	<ul style="list-style-type: none"> Soil Stratigraphy SPT and LPT SCPT DST BPT Index Properties Strength Properties (including Dynamic Testing)
Tetra Tech	2019	TP1 to TSF6 (proposed) Geotechnical Investigation	Becker Hammer (Closed-ended, instrumented) & Sonic	<ul style="list-style-type: none"> Soil Stratigraphy SPT iBPT Index Properties

¹ EP1: Exfiltration Pond 1

An expanded version of Table 2-2, providing additional investigation details, is included as Table A in the Tables section. Table A includes boreholes and/or testpit quantities, specific laboratory tests, and geotechnical instrumentation installed during each investigation. Other selected geotechnical data including laboratory strength testing results are also presented. The geotechnical instrumentation installed in the tailings facilities include standpipe piezometers, monitoring wells, pumping wells, vibrating wire piezometers, and inclinometers.

A compiled list of individual boreholes, associated investigations, and drilling details is provided in Table B of the Tables section.

2.3.2 Laboratory Testing Results

Laboratory testing programs were conducted as part of the geotechnical investigations. Disturbed and undisturbed samples of tailings and foundation soils were tested throughout these programs. Most of the laboratory tests conducted on the foundation soils consisted of standard index property testing (e.g., moisture contents, particle size distributions, hydrometers, specific gravities, and Atterberg limits).

Knight Piesold completed two consolidated undrained (CU) triaxial tests on foundation soils underlying the tailings ponds: one during each of their geotechnical investigations in 2010 and 2011 (KP 2012a). The test specimens were obtained from Boreholes DH10-01 and GH11-03 with Shelby tubes, and both were drilled along the northwestern crest of TP4 (Figure 2-5). SRK conducted a CU triaxial test and a one-dimensional consolidation test following their 2016 geotechnical investigation. SRK also conducted various dynamic and cyclic laboratory tests on re-constituted samples. These included bender element velocity tests, stress-controlled cyclic direct simple shear tests, and post-cyclic monotonic direct simple shear tests. This data was used to assist in the development of the properties assigned to the foundation soils in the analyses. Table A in the Tables section provides a breakdown of the laboratory testing conducted for each geotechnical investigation.

2.4 Survey Coordinate System

The mine site has been surveyed using two coordinate systems. A local, imperial mine coordinate system (MCS) was used for most mine site development. Post-mine operations have been surveyed using the NAD 83 UTM coordinate system. All drawings are presented using the NAD 83 datum. Drawings prepared in the MCS have been transformed using site developed transformation equations, or have been scaled to match known features. For both translocations, historic points and line work are approximate. Surveys completed in NAD 83 are considered accurate to equipment specifications.

Elevations in the MCS are approximately 5 ft. (1.5 m) higher than UTM elevations. All imperial elevations presented in this report are consistent with the MCS datum. Metric elevations have been converted to the NAD 83 datum and reflect the 1.5 m reduction in elevation. It should also be noted that the site transformation equation was based on statistical analysis of a finite number of data points. Subsequent analysis by Tetra Tech (EBA, A Tetra Tech Company 2011) suggest an elevation correction of 2.0 m. For the purpose of this report, the 1.5 m correction used by NATCL has been carried forward for consistency with existing documentation.

3.0 TAILINGS POND DEVELOPMENT

3.1 General

Tailings deposition and pond development histories were compiled from a review of numerous reports, aerial photographs, and recent site investigation results. These included:

- Golder Associates investigation, inspection, and design reports (Golder 1974, 1976a, 1976b, 1976c, 1977a, 1977b, 1980, 1984, 1985a, 1985b, 1985c, 1985d);
- Consol Geotechnical Services inspection and design reports (Consol 1986a, 1986b);

- EBA Engineering investigation, design, and record reports (EBA, 2001a, 2001b, 2001c, 2006, 2007a, 2007b, 2007c, 2007d, 2008b, 2008c, 2009b, 2009c; EBA, A Tetra Tech Company 2013);
- Knight Piesold design and record reports (Knight Piesold 2011, 2012b);
- 2019 annual geotechnical inspection (Tetra Tech 2019b);
- NATCL interim closure and reclamation plan (NATCL 2015); and
- Aerial photos – A12270 (1949), A12278 (1949), A12637 (1950), A171105 (1960), A20849 (1968), A22355 (1971), A24528 (1976), A26158 (1982).

Unless otherwise specified, the information presented in the following sections was compiled primarily from the above-noted reports.

The Cantung tailings ponds are mainly constructed of locally available sands, and gravels, typically sourced from glaciofluvial deposits, either from within the dam footprint or adjacent borrow areas. Earlier tailings ponds (TP1, TP2, and TP3) comprised a simple cross-section of compacted granular fill. More recent tailings pond dams (TP4 and TP5) were designed to incorporate upgradient granular filters and geotextile.

Tailings were produced in the process plant through a series of crushing, grinding, and gravity circuits. The resulting tailings composition was approximately 45% sand and 55% fines (45% silt size and 10% clay size particles). Tailings were pumped as a slurry and deposited subaerially in the tailings ponds to form beaches and decant ponds.

Tailings were discharged as either a total waste stream with a solids content of approximately 17.5% or as segregated waste with coarse and fine fractions of 68.9% and 8.3% solids, respectively. Segregated tailings were produced using a cyclone system with coarse tailings used to construct beach deposits upstream of the dams (for subsequent upstream or centerline construction) or for underground backfilling.

Underground backfilling occurred from 1982 to 1986, and again briefly in 2009. During this time approximately 30% of the coarse tailings stream was diverted to the underground (NATCL 2015). This resulted in a finer blend of tailings being delivered to the tailings ponds over this period and predominantly affected deposition in TP3.

Segregated tailings deposition typically occurred over the summer months with total discharge occurring over winter. Spigot locations were rotated around the tailings ponds to create upstream beaches and reduce ice entrainment in winter.

Total tailings discharge demonstrated segregating behaviour, forming coarser deposits near the discharge location as heavier particles (sand size) fell out of suspension. This appears to have been the predominant discharge methodology later in the mine life, with spigot locations being set to form upstream beach heads with the tailings slimes flowing towards the center of the pond.

Historical plan drawings showing pond development over time have been developed from available aerial photographs and as-built data. TP1 and TP2 development is presented in Figures 3.1-1 through 3.1-4. TP3, TP4, and TP5 development is presented in Figures 3.1-5 through 3.1-14. Additional detail pertaining to tailings deposition and pond development is presented in the CSM.

3.2 Tailings Ponds 1 and 2

TP1 and TP2 are the original tailings ponds on site and are located northeast of most mine infrastructure (Figure 2-3). The TP1 and TP2 dam structures are approximately 17 m and 14 m high respectively with the tailings

cover material flush with the dam crest. The tailings ponds are inspected regularly as part of annual geotechnical inspections and dam safety reviews. The existing condition, as documented in the 2019 annual inspection (Tetra Tech 2019b), is summarized below:

- TP1 and TP2 are decommissioned and were capped with a mixture of granular fill and tailings in the early 1970s.
- The tailings ponds are currently being used as laydown for used tires, some heavy equipment, and some machinery. There are two storage buildings (a metal clad building and a metal quonset hut) on TP1.
- The surfaces of both TPs are flat and generally well-drained, and it is noted that the surface elevation of TP2 is a couple of metres lower than TP1.
- TP1 and TP2 embankments showed no signs of distress and the downstream slopes (slope angle of 1.4H:1V) are partially vegetated with native shrubs, trees, and grass species.
- The embankment crest (crest width of 8 m) appeared to be relatively level with no signs of differential settlement or distress.

TP1 and TP2 were used from approximately 1963 to 1973. Primary deposition occurred prior to the start of TP3 (approximately 1971); however, Golder (1974) indicates the tailings ponds may have been used as late as 1974 to store cooling water prior to discharge to the Flat River.

Though referenced as two structures, historical reporting and aerial photographs suggest the tailings ponds were constructed as a single containment area and raised concurrently. The center berm separating the two tailings ponds appears to have been constructed during the final TP1 raise, to provide additional tailings containment. It does not seem to extend through the entire tailings depth.

The dams are constructed of material sourced largely from the pond footprint or the former borrow area located within the TP3 footprint. They were constructed in stages using materials comprising a mixture of silts, sands, and gravels, with occasional cobbles and boulders (NATCL 2015). Golder (1974) indicates the location of the pond had a surface deposit of organics and muskeg, 0.9 m to 1.5 m thick. The organics were excavated and displaced as construction progressed so that the embankments are supported on granular material (Golder 1974).

TP1 and TP2 were constructed in four and three stages, respectively. The estimated construction sequencing is shown in Figure 3.2-1, and summarized in Table 3-1. Stages 1 through 3 elevations for TP1 and TP2 are slightly different as a result of scaling from historical drawings; however, historical reporting suggests Raises 1 through 3 were completed concurrently. All dam raises were constructed using upstream dam construction.

Table 3-1: Tailings Pond 1 and 2 Construction Sequencing

Raise ID	Year	Tailings Pond 1 Elevation (feet MCS)	Tailings Pond 2 Elevation (feet MCS)	Construction Method	Comments
1	Unknown	3,668	3,667	Upstream	TP1 and TP2 raised concurrently
2	Unknown	3,676	3,681	Upstream	TP1 and TP2 raised concurrently
3	Unknown	3,690	3,691	Upstream	TP1 and TP2 raised concurrently
4	Unknown	3,750	-	Upstream	TP1 raised

The tailings ponds were capped and reclaimed when they reached capacity. Test pitting in the tailings ponds as part of the ESA indicates the cap comprises a mixture of granular fill and tailings.

3.3 Tailings Pond 3

TP3 was operated as the primary tailings deposition facility from 1971 through 2007 (NATCL 2015) and is approximately 35 m in height (ground surface to tailings dam crest). Its location is shown in Figure 2-2. Observations from the 2019 annual inspection (Tetra Tech 2019b) are summarized below:

- TP3 is filled to near crest elevation with tailings and is uncovered.
- Some stockpiled, dewatered tailings from TP5 were placed in the central portion of the facility in 2015 to increase exfiltration capacity in TP5.
- Side slopes were measured between 33° and 37° and showed no signs of deformation. The crest of the dam (approximately 5 m wide) was flat with no signs of settlement or distress.
- Some minor erosion gullies were observed on the south and east side slopes of TP3 that are starting to be filled in with wind blown tailings.
- The mine typically adds water to the tailings surface to reduce wind blown tailings. NATCL has previously run an irrigation system to water the surfaces of TP3, TP4, and TP5. The system was functioning over the summer but had been decommissioned for the winter at the time of the site visit.
- In summer 2019, NATCL applied calcium chloride (CaCl) to the tailings surface as a dust suppressant measure. In the fall, NATCL also applied Soiltec soil stabilizer as a dust control agent over the surface of the TP3 exposed tailings.

TP5 tailings stockpiled on TP3 were intended to be moved to a newly commissioned dry stack tailings facility in proposed TSF6; however, the mine went into care and maintenance before the dry stack facility could be constructed and the tailings relocated.

TP3 represents the largest tailings containment structure at the Cantung Mine. Locally available, sands and gravels were utilized in the construction of the 35 m high dam. TP3 was started in 1971 (Golder, 1974), with an initial dam crest elevation of 3,670 ft. (MCS). Successive dam raises have increased the TP3 crest elevation to 3,765 ft. (MCS).

Historical imagery shows that the TP3 footprint was used as a borrow source prior to pond development. The excavation depth is uncertain, but the lateral extents can be seen on the 1960 and 1968 plan drawings (Figures 3.1-5 and 3.1-6). This was largely in the glaciofluvial slope material identified in Tetra Tech's terrain assessment (see Section 4).

Golder (1974) indicates the initial pond was constructed with locally available material from within the pond footprint. The borrow source then appears to have shifted to the Ski Hill borrow area around 1976 based on aerial imagery and information reported in Golder (1976c). By 1980 the TP5 footprint was also being used as a borrow source (Golder 1980).

Golder (1976c) notes that no shallow silty/organic material was observed at the original ground interface during drilling; suggesting that the ground surface was stripped prior to construction or these materials were not present to begin with. The footprint for subsequent widening may not have been grubbed (Golder 1980). Golder (1980) notes the presence of thin bush vegetation underlying the 1980 widening but did not expect dam performance to be impacted.

TP3 was raised 11 times over the course of operations. The approximate raise elevation and construction method is summarized in Table 3-2. The construction sequence is presented in Figure 3.2-2.

Table 3-2: Tailings Pond 3 Construction Sequencing

Raise	Year	Raise Elevation (feet MCS)	Construction Method	Comments
-	1971	3,670	-	-
1	1972	3,680	Downstream	-
2	1973	3,691	Downstream	-
3	1974	3,697	Upstream	-
4	1976	3,703	Upstream	-
5	1977	3,713	Centerline	Material added downstream to widen berm
6	1980	3,725	Centerline	Material added downstream of Raise 5 to widen dam.
7	1984	3,742	Centerline	-
8	1986	3,750	Centerline	Constructed with material from the downstream side of dam
9	2001	3,756	Upstream	Constructed with material from the downstream side of dam
10	2003	3,761	Upstream	-
11	2005	3,765	Upstream	-

Historical reporting shows some discrepancy in the upstream slope angle for the initial dam construction and subsequent two raises. Early reports (Golder 1974) show flatter interior slopes, but all subsequent reporting (Golder 1976c, Consol 1986a, and EBA 2001a) indicated steeper interior side slopes.

Material for Raise 8, and possibly Raise 9, were sourced from the downstream dam slope, resulting in a step at approximate Elevation 3,735 ft. (MCS).

The dam was widened on its downstream side in 1976 and 1980 to improve the overall stability. This reduced the proportion of dam raises that were constructed directly over upstream tailings. The exceptions to this are Raises 9, 10, and 11 which were constructed as upstream raises.

EBA (2009b) notes that portions of the TP3 surface were capped in 1993 with till to control the dust. The extent and thickness of the cover is unknown. This material was subsequently covered with tailings as part of continued operations.

3.4 Tailings Pond 4

TP4 is located north of TP3 as shown on Figure 2-2 and is approximately 35 m in height (ground surface to tailings dam crest). It was originally used as an exfiltration pond until 2007 when it was converted to a tailings deposition area and TP5 was established as an exfiltration pond. Observations from the 2019 annual inspection (Tetra Tech 2019b) are summarized below:

- TP4 is filled to the crest with tailings and not in use. The tailings surface is uncovered.

- The embankment slopes (slope angle of 2H:1V) showed no evidence of cracking, bulging, or slumping. The embankment crest appeared to be relatively level with no signs of distress or differential settlement.
- The ditch at the toe of the dam was dry at the time of the inspection.
- Interceptor ditches upslope of the facility are operating as designed, directing upslope runoff to the north side of the facility
- In summer 2019, NATCL applied CaCl to the tailings surface as a dust suppressant measure and in the fall NATCL also applied Soiltec soil stabilizer and dust control agent over the surface of the TP4 exposed tailings.

TP4 operations began in the early 1970s. It served as an exfiltration pond until the accumulation of fine sediment prevented its continued operation. In 2007, TP4 became the primary tailings storage cell and TP5 was used as the exfiltration pond. This containment facility was used until 2013 and contains an estimated 850,040 m³ of material (NATCL 2015).

Prior to its conversion to a tailings pond, TP4 was dredged in autumn 2006 in an attempt to improve its exfiltration capacity (EBA 2007b). The dredging was unsuccessful, as fines were found to have migrated into the foundation soils to a depth of at least 2.4 m, essentially blinding off any exfiltration capacity. Material from dredging operations was dumped in the TP5 footprint. The dredge spoil is shown on the 2007 plan drawings (Figure 3.1-12).

TP4 was raised in four stages using upstream construction. The generalized cross-section is shown in Figure 3.2-3. The geometry comprises a 300 mm minus granular core (14 to 32 m wide) with a 75 mm minus upstream graded filter. The upstream face of the raise was lined with nonwoven geotextile. The portion of the raise constructed over beached tailings was subcut and constructed on a geotextile wrapped waste rock or pit run layer. The TP4 construction sequencing is summarized in Table 3-3.

Table 3-3: Tailings Pond 4 Construction Sequencing

Raise	Year	Raise Elevation (feet MCS)	Construction Method	Comments
-	-	3,690	Upstream	Existing exfiltration berm
1	Early 2007	3,715	Upstream	-
2	Late 2007	3,730	Upstream	-
3a	2009	-	-	Interim construction of upstream portion of Stage 3 raise. No change in elevation
3b	2010	3,742.5	Upstream	-
4	2011	3,757	Upstream	-

Golder (1976c) did not observe organics in the boreholes, suggesting the footprint of the exfiltration pond was grubbed prior to construction. The general cross-section for the exfiltration berm is unknown; however, construction photographs from the Stage 1 raise (EBA 2008b) show a granular berm with geotextile on its upstream face.

Golder (1976a) noted that the TP4 area was previously used as a borrow area and as a landfill for mill fire refuse. BH's 20, 20A, and 21 were drilled through the embankment to confirm the presence of mill waste; however, nothing was encountered in the boreholes. During construction in 2007, debris was encountered within the pond footprint. EBA (2007c) completed a magnetometer survey to delineate the debris and the debris was removed during construction.

3.5 Tailings Pond 5

TP5 (approximately 16 m high from ground to dam crest) was originally designed as a tailings retention dam but was changed to an exfiltration pond when TP4 stopped working. Observations from the 2019 annual inspection (Tetra Tech 2019b) are summarized below:

- All sides of TP5 were observed to not show signs of deformation.
- The embankment crest (8.5 m wide) displayed no signs of distress or differential settlement. There were no signs of seepage from the tailings at the abutments on the downstream face (2.5H:1V) or downstream toe.
- In summer 2019 NATCL applied CaCl to the tailings surface as a dust suppressant measure and in the fall NATCL also applied Soiltec soil stabilizer and dust control agent over the surface of the TP5 exposed tailings.
- The interceptor ditch above TP5 was dry and clear at the time of the inspection. There was no evidence of areas of ponding, although that can be difficult to evaluate in dry conditions.

Originally designed as a tailings solids storage facility, TP5 would have provided a storage capacity of 153,000 m³. In 2007, changes to the tailings management plan conscripted TP5 to be the primary exfiltration pond. TP5 was then used as the primary tailing storage facility in 2013 because TP4 was full to design capacity. There have been three raises to TP5's dam to bring the current capacity to 587,000 m³ (NATCL 2015).

TP5 construction began in 1986, shortly before the mine shutdown (Consol 1986b). As of August 1986, the dam base had been cleared of disturbed material, and approximately 1.2 m of granular fill had been placed.

In the summer of 2006, TP5 was constructed to a crest elevation of 3,740 ft. (MCS) (EBA 2007b). This is less than the design elevation of 3,760 ft. (EBA 2006) but is consistent with the initial crest elevation recommended in Golder (1985a). The generalized cross-section comprises a 400 mm minus material used as central structure (30 m wide), a 75 mm (15 m wide) upstream filter, and a 900 mm minus downstream toe berm (11 m wide and 3 m high). The dam was raised to 3,743 ft. in 2010, and to 3,750 ft. in 2011 (KP 2011). A fourth raise to 3,760 ft. was completed in 2012 (EBA 2013) and the final raise to 3,782 ft. completed in 2015 (Tetra Tech EBA 2015). The TP5 construction sequencing is summarized in Table 3-4.

Table 3-4: Tailings Pond 5 Construction Sequencing

Raise	Year	Raise Elevation (feet MCS)	Construction Method	Comment
1	2006	3,740	Centerline	-
2	2010	3,743	Centerline	-
3	2011	3,750	Centerline	-
4	2012	3,760	Centerline	-
5	2015	3,782	Centerline	Dam raise above original design elevation

4.0 SUBSURFACE CONDITIONS

4.1 Surficial Geology

4.1.1 Depositional History

Tetra Tech completed a terrain analysis based on air photograph interpretation for the site. This involved a review of geotechnical investigation reports and a field program to define soil texture and ground truth the terrain assessment. The terrain analysis built on previous works completed by BGC Engineering Inc. (as cited in SRK 2017a) and Stantec (2014).

Natural terrain units within the developed area were mapped using historical air photos from 1949 and 1950 (1:40,000 scale photos). The completed terrain map is presented in Figure 4-1. This scale is not optimum for terrain mapping (typically 1:20,000 or larger scale is preferred); however, the photo quality was good and, with magnification, allowed more detailed interpretation and identification of geomorphological features and depositional boundaries between surficial materials of different genesis. The stratigraphy below the mine production and tailings deposition areas is typical of regional montane deglaciation, with sequences of advance and recession of valley glaciers probably between 10,000 and 15,000 years ago. Basal and lateral till is deposited during periods of glacial advance. High-energy fluvial deposition from rapid melting during glacial recession typically results in glaciofluvial material over the till deposits. Glacial meltwater can erode and transport till deposits, contributing to unclear differentiation and similarity of glacial till and glaciofluvial material in some cases. Where reliable textural descriptions are available, this information is preferable to assumptions based on material genesis.

Terraces (FGt) and kettling (-H), observed from air photograph interpretation of pre-development terrain, underlying the tailings ponds are defining features of glaciofluvial deposition. Glaciofluvial terraces on lower valley slopes, such as those underlying TP3 and TP4, are commonly eroded by recessional glacial rivers or Quaternary fluvial activity, resulting in escarpment slopes (FGka), defining the outer boundary of the terrace polygon. Glaciofluvial terraces with glacial meltwater channels (FGt-E) eroded into the surface are mapped at the base of slopes.

In their desktop geomorphology study, BGC (as cited in SRK 2017a) reported that there is more glaciofluvial material and less alluvial material underlying the tailings ponds than was previously suggested by SRK's (2017a) borehole logs. This conclusion is supported by Geological Survey of Canada (GSC) mapping (Dyke 1990), the desktop terrain mapping conducted by Stantec (2014), and Tetra Tech's (2020c) field mapping and ground truthing.

It is unlikely that there will be significant presence of fine-textured soil upslope of the valley floor. No glacial lake sediments were mapped in the upper part of the Flat River near the mine (Dyke 1990). As stated in BGC (as cited in SRK 2017a): "This, however, does not imply the complete absence of such sediments, which may be sporadic and associated with localized, short-lived ponding." Lateral moraine could also be a soil component within the areas mapped as glaciofluvial, with similar texture but more variable, and could contain silt in layers of the matrix.

Borehole logs have demonstrated evidence of fine-textured soils (silt) associated with localized ponding or periods of low energy glaciofluvial deposition.

4.1.2 Soil Types and Occurrences

Five native soil types have been identified on site: colluvium, glacial till, glaciofluvial, fluvial, and organic. A significant proportion of the surficial material on middle to upper valley slopes is bedrock or frost-shattered rock. Fill has also been identified in many of the disturbed areas around site.

The following list outlines the surficial material types and observations of their occurrence on site:

- **Colluvium** is naturally occurring, loose, unconsolidated sediment deposited at the lower parts of hillslopes by either rainwash, sheetwash, slow continuous downslope creep, or a variable combination of these processes. Much of the colluvium originates from frost-shattered rock on high mountain slopes, so the fragments are typically angular, with little evidence of erosion or long-distance transport (rounding). The new borrow pit developed across the Flat River from the townsite exploits a large colluvial fan.
- **Glacial till**, deposited under or proximal to glacial ice, is typically deposited on lower to mid-valley slopes. Much of the till observed is somewhat indistinct from glaciofluvial material and some may have been redeposited or redistributed by water during deglaciation.
- Large deposits of **glaciofluvial material** are common and provide a good source of loose, granular material suitable for construction and fill. Quaternary (post-glacial) **fluvial material**, mostly along the Flat River, consists of rounded to sub-rounded washed gravel, cobbles, and boulders, and can be a local source of fill.
- **Organic soils** have developed in the floodplain of the Flat River. Due to their proximity to the Flat River riparian corridor, no organic deposits have been identified as suitable borrow sources. It is expected that stockpiles of organic-rich topsoil stripped during development of future borrow sources and other infrastructure will be used for cover where revegetation is prescribed.
- **Bedrock** outcrops sporadically along the base of the hillslopes adjacent to the main mine site, and more continuously at higher elevations.
- **Fill materials** on site consist mainly of sand and gravel, with trace silt and occasional cobbles and minor inclusions of wood fragments, plastic, and/or metal debris. They have been sourced from local native materials (colluvium and Flat River flood plain deposits) and waste rock, and are compositionally similar to those materials. Fill materials are found over the disturbed areas of the mine site and have been reworked and moved multiple times during the mine life.

4.2 Groundwater

Tetra Tech assessed groundwater elevations around the mine site from monitoring well data collected during two Environment Site Assessment (ESA) field programs in 2017 and 2018 (Tetra Tech 2020a). Groundwater elevations were measured at 52 monitoring well locations. The wells are typically clustered around the crests and toes of the dam structures, although some shallow wells were installed in TP1/2 as part of the TCAMP program. The available groundwater data was used to develop an inferred groundwater contour map across the mine site and townsite areas including the tailings pond facilities (Figure 4-2).

The groundwater contours in Figure 4-2 were used as the baseline groundwater elevations for stability and deformation analysis, which are shown on the geological model plots presented in Section 5.0. The data from the ESA represents a consistent time stamp for the data, which was why it was used as a baseline.

Additional groundwater elevation data has been measured in historical boreholes and monitoring wells with variable record lengths. Vibrating wire piezometers have also been installed in TP3, TP4, and TP5, and provide groundwater data, particularly under the dam foundations. A list of historical instrumentation locations is provided in Table C of the Tables section and shown on Figure 4-3a and Figure 4-3b.

The available groundwater data was reviewed to assess potential for fluctuations in the baseline groundwater elevations. These are indicated on the geological model plots discussed in Section 5. In several cases, groundwater elevations are available at a single point in time or over a short duration. As such, these measurements may not accurately reflect the true range of groundwater elevations. Furthermore, some groundwater elevations were

collected prior to tailings dam construction and the potential influence of tailings deposition on groundwater contours is not reflected in these measurements.

4.3 Permafrost Conditions

The mine site is located in the Logan Mountains Ecoregion (Ecosystem Classification Group 2010), within the extensive discontinuous permafrost (50% to 90%) (EI zone). Such areas are characterized by rugged terrain and perpetual snow fields at higher elevations, according to the Canada Permafrost Map (Department of Energy, Mines and Resources 1995). In such settings, surficial materials are underlain by extensive discontinuous permafrost and areas of low ground ice content (less than 10%) in the upper 10 m to 20 m of natural ground.

Previous investigations have identified limited and isolated permafrost at the site. During the 2017 field program, frozen ground was encountered at the existing mine waste rock pile outside the main portal adit and again in 2019 during waste rock excavation for ramp construction. Permafrost was encountered 4.8 m below ground surface in the 2017 program, and deeper during the 2019 work. Given the disturbed nature of the waste rock deposition, this depth is not considered indicative of active layer thicknesses where permafrost may exist.

Frozen ground was identified in TP1 and TP2 during testpitting; however, this was likely isolated ice lensing formed during winter tailings deposition and not a reflection of permafrost aggradation in the tailings ponds. Subsequent drilling indicates unfrozen foundation ground conditions adjacent to the tailings dams. Groundwater wells are typically unfrozen year round, further substantiating the largely unfrozen conditions in and around the tailings ponds.

The risk of frozen tailings is that, during thaw, large quantities of water could be released resulting in elevated moisture contents and increased liquefaction risk. This condition is expected to be relatively short lived at Cantung since the tailings are relatively free draining. Potential increases in moisture and groundwater elevation was evaluated as part of the FLAC sensitivity analyses and found to have some effect on pond performance; however, the larger driver was liquefaction of the foundation soils underlying the dam.

With the exception of isolated pockets of frozen ground at select locations, the site can largely be assumed to be underlain by unfrozen ground conditions.

5.0 GEOLOGICAL MODEL

5.1 Model Development

Tetra Tech developed a geological model for the tailings ponds by integrating data from historical geotechnical investigations (summarized in Table 2-2), pre-development terrain mapping, and compiled reports (Section 3.0). Interpretation of the data was often required while comparing multiple sources due to new understanding of the local stratigraphy and depositional history. Geological cross-sections are presented in Figures 5-1 through 5-11. Cross-section locations are shown on Figures 2-4 through 2-6.

Cross-sections perpendicular and parallel to the dam crest alignments were selected to capture and characterize ground conditions underlying the tailings ponds. Perpendicular sections provide detail through the dam structure and tailings, and parallel sections help assess changing conditions between perpendicular sections. Cross-sections were also selected to mirror previous evaluations and allow for comparison of results.

Soil units shown in the sections were delineated from the review of borehole log descriptions, material testing, and terrain mapping. Distinct surface features identified on the pre-development air photographs provide a high level of

confidence in the genesis of surficial materials underlying the tailings ponds. Drill logs provide good stratigraphic definition between distinct units; however, clear delineation between fluvial and glaciofluvial boundaries was challenging. Drill logs were completed by various personnel and multiple consulting firms, and descriptions of the subsurface material typically did not include textural details that would normally be used by a geomorphologist to aid in genesis determination. Earlier studies came to similar conclusions: “Details such as clast rounding, density and layering were not consistently described in all of the logs.” and “substantial uncertainty prevails in the true genesis of materials” (BGC as cited in SRK 2017a). “The distinction between fluvial and glaciofluvial materials in this area is highly subjective” (Stantec 2014). For analysis, conservative strength parameters were assigned to these units to reflect the uncertainty in the delineation. That said, the primary failure mechanism relates to post-seismic shears strengths which were evaluated directly from iBPT and CPT results. This data reflects direct in situ measurements regardless of material genesis. The associated failure analysis does not require precise delineation of the fluvial and glaciofluvial deposits. The uncertainty in the unit boundaries is therefore not expected to materially impact the analysis results.

For the geotechnical evaluation, the model focused on the embankment configuration, foundation stratigraphy, and general tailings properties. The primary driver for pond instability is liquefaction of foundation soils, so delineation of tailings stratification was not considered in detail. Broad observations such as the placement of upstream cyclone tailings have been included on the generalized cross-sections (Figures 3.2-1 through 3.2-3).

Liquefiable foundation soils were identified at TP1, TP2, TP3, and TP4 (Section 8). The lateral and vertical extent of the liquefiable soils varied significantly between cross-sections and individual boreholes, particularly at TP1 and TP2. Additional cross-sections showing the interpreted liquefiable zones were prepared and are presented in Appendix D. These plots form the basis of the stability analyses discussed in Section 9.0.

5.2 Interpreted Conditions

5.2.1 Tailings Ponds 1 and 2

The interpreted soil conditions underlying TP1 and TP2 are presented in Figures 5-1 through 5-3. Terrain mapping (Figure 4-1) indicates that TP1 generally overlies colluvium sourced from the south valley slopes, and TP2 is constructed over glaciofluvial deposits. The Flat River alignment adjacent to the tailing ponds appears to be constricted by the colluvial fan underlying TP1 and colluvial fans originating from the north valley slopes. The river alignment through this area follows a sinusoidal flow path that predates construction of the tailings ponds (Figure 3.1-1). The glaciofluvial/fluvial interface extends under the TP2 dam crest, and under the colluvium within the TP1 footprint.

Section A through TP1 (Figure 5-1) shows the fluvial deposits extending slightly upstream of the dam crest, consistent with the terrain assessment. Colluvium overlies the fluvial materials and extends upgradient towards the south valley slope. Both the colluvium and fluvial deposits are underlain by glaciofluvial material which extends southwards to edge of mine site development (see Figure 4-1).

Section B through TP2 (Figure 5-2) comprises fluvial material overlying glaciofluvial deposits, consistent with the terrain assessment. The fluvial material appears to extend slightly farther past the crest than at TP1.

Bedrock underlying the tailings ponds is deep (greater than 30 m to 40 m) and appears to shallow somewhat (25 m to 30 m) upgradient of the dam. There is limited bedrock data beyond the crest of the dam; however, data from townsite and TP4 boreholes suggest a general increasing of bedrock elevation towards the glaciofluvial and valley slope (Mka-V) interface. Given its relatively small footprint and distance from the valley slope interface, bedrock underlying TP1 and TP2 is expected to be relatively deep.

Groundwater is generally located under the tailings, below original ground. The groundwater contours generally run parallel to the surface contours, as shown in Figure 4-2, daylighting in the Flat River.

As noted in Section 3.0, the tailings ponds appear to have been constructed concurrently, as evidenced in Figures 3.1-2 and 3.1-3. The centerline berm separating the pond appears to have been constructed to facilitate the raising of TP1 above TP2 (Figure 3.1-4).

5.2.2 Tailings Ponds 3, 4, and 5

The interpreted soil conditions underlying TP3 and TP4 are presented in Figures 5-4 through 5-11. The terrain assessment (Figure 4-1) shows the tailings ponds generally overly glaciofluvial materials with fluvial material encroaching on the downgradient portion of the dam. The upgradient edge of the tailings ponds roughly intersects with south valley slope.

The Flat River alignment is less constricted than adjacent to TP1, with exception of a colluvium fan on north valley slope which constricts the river alignment downgradient of TP4.

The generalized stratigraphy comprises glaciofluvial material underlain by till. Fluvial deposits overly the glaciofluvial material under the dam footprint. With the exception of Section G (Figure 5-8), fluvial materials do not typically extend upstream of the dam crest. In Section G fluvial materials extend along a significant portion of the profile, suggesting a possible former tributary or a misinterpretation of the fluvial/glaciofluvial interface.

Bedrock is 25 m to 35 m below the ground surface at the toe of the dam and gradually rises towards the intersection with the south valley slope, particularly along TP4. Boreholes drilled on the upgradient edge of TP4 at Section D (Figure 5-5) show bedrock as shallow as 2 m below ground surface.

Groundwater contours typically follow surface contours as shown in Figure 4-2. Groundwater elevations are typically below the tailings base, in the original ground.

6.0 DESIGN GUIDELINES

6.1 Dam Classification

As noted in the most recent Dam Safety Review (SRK 2017b), TP1 to TP5 have been classified as “Significant Consequence” based on the Canadian Dam Association guidelines (CDA 2013). Table 6-1 provides the consequence classifications given to the tailings ponds in past dam safety reviews (taken from SRK 2017b).

Table 6-1: Summary of Dam Classification of Existing Tailings Facilities (after SRK 2017b)

Company	Year	Guideline	Tailings Pond(s)	Dam Consequence Classification	Comments
EBA	2007	CDA 1999	TP4 and TP5	High	Classification for TP4 and TP5 based primarily on the financial impact of a dam failure on mine operations, site specific conditions, and the observations of the dam safety reviewers (SRK 2012) at this time. TP3 was not classified.
EBA	2008	CDA 2007	TP4 (Stage 2 Construction)	Significant	MVLWB rejected Stage 2 construction of TP4 requesting a “High” DCC, based on the impacts to the Flat River system and based on past classifications.
EBA	2008	CDA 2007	TP4 (Stage 2 Construction)	Significant	MVLWB approved Stage 2 construction of TP4.
EBA	2008	CDA 2007	TP4 (Stage 3 Construction)	Significant	MVLWB rejected Stage 3 construction requesting a “High” DCC.
EBA	2009	CDA 2007	TP4 (Stage 3 Construction)	Significant	MVLWB approved Stage 3 construction. MVLWB recognized that to meet a High DCC would require a buttress which would impact the fish habitat in the Flat River.
Knight Piesold	2011	CDA 2007	All	Significant	KP Tailings Management Plan adopted the Significant DCC.
SRK	2012	CDA 2007	All	Significant	In the 2012 Dams Safety Review, SRK accepts the Significant DCC for TP3 and TP4.
SRK	2017	CDA 2016	All	Significant	-

6.2 Review of Design Guidelines for Tailings Dams

The CDA provides guidelines for earthquake loadings and stability of tailings facilities (CDA 2013 and 2014) and were reviewed to develop evaluation criteria. Mining Association of Canada guidelines (MAC 2019) were also reviewed; however, this document provides general guidelines for planning and developing tailings management frameworks, but not for specific evaluation criteria.

The CDA guidelines recommend the assessment of the slope stability using limit equilibrium analysis and, when necessary, using finite element or finite difference analyses to predict deformations and porewater pressures in certain situations.

6.2.1 CDA Guidelines

The 2014 CDA guidelines recommend that stability analysis be based on either worst-case values for input variables, or nominal values with a safety factor applied to the results. The analysis performed herein considered both cases in order to provide a conservative assessment of these facilities.

A summary of the recommended earthquake loading is provided in Table 6-2 (CDA 2014).

Table 6-2: CDA Recommended Earthquake Loadings (from Table 4-2: Target Levels for Earthquake Hazards, Standards-Based Assessments for Closure – Passive Care Phase)

Dam Class	Annual Exceedance Probability (AEP) - Earthquake ⁽¹⁾
Low	1 in 1,000 years
Significant	1 in 2,475 years
High	Average between 1 in 2,475 years ⁽²⁾ and 1 in 10,000 years AEP or MCE ⁽³⁾
Very High	1 in 10,000 years AEP or MCE ⁽³⁾
Extreme	1 in 10,000 years AEP or MCE ⁽³⁾

⁽¹⁾ Mean values of estimated range in AEP levels for earthquakes should be used. The earthquakes with AEP as defined above are input as the contributory earthquake to develop the Earthquake Design Ground Motion.

⁽²⁾ This level has been selected for consistency with seismic design levels given in the National Building Code of Canada.

⁽³⁾ Maximum credible earthquake (MCE) has no associated annual exceedance probability (AEP).

The recommended target factors of safety defined by CDA are summarized in Table 6-3. The CDA indicates that these values are considered acceptable for all phases of a tailings dam, including active and passive closure. Values for during/end of construction were not considered as the dams are currently in the long-term state post construction. Full or partial rapid drawdown factors were not considered as the water levels in the tailings ponds are already low.

Factors of safety (FS_{slope}) represent a measure of slope stability and are defined as the ratio of those forces resisting slope movement to those forces causing movement. They provide a level of conservatism to account model inaccuracies, knowledge of stratigraphy, and uncertainties in soil parameters. A FS_{slope} less than 1 indicates a potential for slope instability whereas a FS_{slope} greater than 1 are less susceptible to slope instability. The selection of appropriate FS_{slope} depends on several factors including loading duration and confidence in material properties.

The FS_{slope} in Table 6-3 provide recommended minimum FS_{slope} for several loading conditions.

- Static: Geotechnical stability loading condition that considers the existing slope condition without ground acceleration due to an earthquake;
- Pseudo-static: Stability loading condition that considers forces generated during an earthquake event; and
- Post-seismic: Stability loading condition that considers modified strength parameters resulting from earthquake activity.

The variable FS_{slope} presented in Table 6-3 (for closure conditions) reflect the likelihood of occurrence and severity of its consequence. Typically, more frequent loading condition or higher consequence events would be assigned a higher FS_{slope} .

Table 6-3: CDA Recommended Target Factors of Safety for Operation, Transition, and Closure Phases (from Tables 3-4 and 3-5, CDA Technical Bulletin, 2014)

Loading Condition	Minimum Factor of Safety
Static – long term (steady-state seepage)	1.5
Pseudo-static (during earthquake shaking)	1.0
Post-earthquake	1.2

It should be noted that FS_{slope} are intended to ensure an acceptable level of service for the design loading condition; however, some deformation can be expected even if FS_{slope} exceeding 1 are attained.

6.2.2 Basis of Evaluation

The CDA guidelines have been adopted for the geotechnical evaluation. The guidelines provide a more conservative set of evaluation criteria and are considered suitable given the heterogeneity observed in soil conditions.

Potential reductions in factors of safety may be considered for remedial options where aggregate cross-sections representing conservative soils profiles (such as Section A-A₂ discussed in Section 9) are applied to the analysis. However, the factors of safety recommended in Table 6-5 have been applied as a starting point for analysis.

Factors of safety provide a relative measure of slope stability; however, they don't specifically address failure consequence. As such, deformation analyses have been included to help quantify the "what if" question. This applies particularly to the existing tailings ponds configuration where no modifications or stabilization measures are provided.

6.2.3 Declassification

The following analysis treats the impoundment structures as tailings dams, and applies the FS_{slope} discussed above; however, CDA guidelines (CDA 2014) do allow structures to be declassified and treated as waste piles provided it can be demonstrated that the material contained by the dam is not liquefiable. This requires consideration of:

- Degree of saturation;
- Impact of ponded water on stability; and
- Potential for piping.

Additional information and assessment would be required to determine if the tailings dams could be declassified.

7.0 SITE-SPECIFIC SEISMIC HAZARD ASSESSMENT

The recommended earthquake loadings from the 2014 CDA guidelines for mining dams were used for the seismic analysis. According to Table 4-2 of the 2014 CDA guidelines (reproduced in Table 6-2 above), the target earthquake hazard level for a Significant class dam in the passive care (closure) phase is an AEP of 1 in 2,475 years.

For the previous liquefaction and stability assessments undertaken by SRK (2017a), the seismic hazard parameters for the site were obtained from the 2010 National Building Code of Canada (NBCC 2010), which gives a peak ground acceleration (PGA) of 0.245g for the 2,475-year event. The 2015 NBCC hazard maps show a reduction in the hazard level at this location, with a PGA of 0.157g.

As noted in the CDA guidelines, the national hazard maps generated for the NBCC are not site-specific and may not be appropriate for remote sites. Accordingly, the guidelines recommend that a site-specific seismic hazard assessment be conducted based on: "(i) local and regional geotectonic information; and (ii) a statistical analysis of historical earthquakes experienced in the region, taking into account all potential seismic sources capable of contributing significantly to the seismic hazard at the site" (CDA 2013).

To address the above requirements, Tetra Tech retained Onur Seeman Consulting Inc. (OSC) to conduct a probabilistic seismic hazard assessment (PSHA) for the site. OSC's report is provided as Appendix B. The PSHA was carried out using GSC's fifth generation seismic hazard model as a base model, with several changes introduced to better characterize the seismic activity at the site. The resulting hazard was found to be higher than the 2015 NBCC values for short periods and lower for long periods, with a PGA of 0.210g for the 2,475-year event. Based on the deaggregation of the hazard for the PGA, spectral acceleration for a period of 0.2 s (SA(0.2s)), and spectral acceleration for a period of 1.0 s (SA(1.0s)), a mean moment magnitude (M_w) of 6.54 was used for Tetra Tech's liquefaction assessments (Section 8.0).

As part of the seismic hazard assessment, OSC produced a suite of 11 ground motion time histories to be used for the seismic analysis of the tailings facilities. The records were selected from the PEER NGA-West2 database and scaled to match the 2,475-year uniform hazard spectrum (target spectrum). The selected records are summarized in Table 7-1.

Table 7-1: Selected Ground Motion Time Histories

ID	Event	M_w	Station	R_{rup}^1 (km)	V_{s30}^2 (m/s)	Duration (s)	Scale Factor
IV	Imperial Valley, 1979	6.5	CPE	15	472	64	1.0
CO1	Coalinga, 1983	6.4	PG3	39	511	60	1.2
CO2	Coalinga, 1983	6.4	SC3	34	565	60	1.5
MH	Morgan Hill, 1984	6.2	CLS	23	462	28	2.5 ³
CV	Chalfant Valley, 1986	5.8	BPL	15	585	40	1.5
WN	Whittier Narrows, 1987	6.0	SYL	42	440	40	3.0
NR1	Northridge, 1994	6.7	CYP	31	367	30	1.3
NR2	Northridge, 1994	6.7	UCL	22	398	60	1.0
SM	Sierra Madre, 1991	5.6	LAC	26	365	65	2.8
NI1	Niigata, Japan, 2004	6.6	FKH21	31	365	180	1.0
NI2	Niigata, Japan, 2004	6.6	NIG016	32	370	172	1.8

¹ Distance to rupture surface.

² Average shear wave velocity in the top 30 m of soil (used for site classification).

³ In addition to scaling, this record was spectrally modified at six periods.

8.0 LIQUEFACTION ASSESSMENTS

Simplified liquefaction triggering assessments were performed for the 2019 iBPT borehole locations at TP1 to TP5 and proposed TSF6. The analyses incorporated the updated seismic input data, discussed in Section 7.0, as well as relevant in situ test data from the historical geotechnical investigations listed in Table 2-2. Details of the calculation methodology are provided in Section 8.1 below, and the main analysis results for each tailings pond are presented in Section 8.2. A supplementary study to assess the liquefaction potential of saturated or nearly saturated tailings that may exist above the interpreted groundwater level is presented in Section 8.3.

8.1 Methodology

8.1.1 Site Response Analysis

One-dimensional seismic ground response analyses were performed using the computer program SHAKE2000 (Ordonez 2011) based on the equivalent-linear, total stress method. The purpose of the analyses was to estimate the amplification or de-amplification of horizontal ground motions propagating through the soil strata and to obtain cyclic shear stress profiles for the liquefaction triggering assessment.

Soil profiles and groundwater levels for each analysis location were defined based on the updated geological cross-sections developed in Section 5.0. The geotechnical input parameters required in SHAKE2000 include shear wave velocity (V_s), modulus degradation (G/G_{max}) relationships, damping parameters, and unit weight. The geotechnical parameters were derived from borehole soil descriptions, downhole shear wave velocity measurements, and seismic cone penetration test (SCPT) data from the various geotechnical investigations. At the interpreted depth of bedrock, the elastic half-space was assigned a V_s of 1,100 m/s, which is a typical value for Site Class B (rock) as per the NBCC (2015).

The main analyses presented in Section 8.3 were conducted based on the interpreted ground conditions and tailings pond configurations at the time of geotechnical investigation (Tetra Tech 2019). Additional site response analyses were performed to assess the liquefaction potential of saturated tailings that may exist above the interpreted groundwater levels across the site. For these analyses, an elevated groundwater level was assigned at the estimated elevation where tailings saturation may exceed 85%. Details on the selection of the groundwater levels within the tailings are provided in Section 8.3.

The modulus degradation and damping relationships were selected for the soil profiles based on material type as follows:

- Fluvial and glaciofluvial soils: Seed and Idriss (1970) curves for sand (upper bound modulus degradation, and lower bound damping).
- Till-like soils: EPRI (1993) for deep cohesionless soils.
- Bedrock: EPRI (1993) for rock.

The 11 earthquake motions provided by OSC (2019) were input as outcropping motions at the base of the soil column. A uniform scaling factor of 0.8 was applied to convert the ground motions from Site Class C (very dense soil/soft rock) to Site Class B (rock), for compatibility with the stiffness properties assigned to the bedrock.

For each analysis location, an average cyclic shear stress profile obtained from all records was used for the liquefaction triggering assessment.

8.1.2 Liquefaction Potential

A liquefaction triggering assessment was undertaken following the approach outlined by Boulanger and Idriss (2014), referred to herein as BI-2014. The cyclic demand, in the form of the Cyclic Stress Ratio (CSR), was calculated based on the average shear stress profiles obtained from the SHAKE2000 analyses described above. The soil resistance to liquefaction, in the form of the Cyclic Resistance Ratio (CRR), was evaluated from the in situ measurement data as follows:

- **iBPT:** Equivalent SPT N_{60} values obtained from the iBPT boreholes (Tetra Tech 2019) were used. Correction factors were applied to account for stress level and fines content based on test data from the corresponding

sonic boreholes. The iBPT results were treated as the main source of information on soil density for this assessment.

- **SPT and LPT:** These were obtained primarily from SRK's (2017a) boreholes. Correction factors (e.g., hammer energy, borehole diameter, and fines content) were applied to the measured N-values.
- **SCPT:** These were obtained from Knight Piesold's (2011) investigation, with corrections applied for fines content.
- **BPT:** SRK's (2017a) interpreted N_{60} profiles from the BPT data were used, which were based on the Sy & Campanella (1993) correlation method and selected Pile Driving Analyzer (PDA) test results. Different BPT correlation methods (e.g., Harder and Seed 1986) may produce substantially different results, which in turn may have a significant impact on the liquefaction assessment. Therefore, these results are presented for comparison purposes only.
- **DST / V_s :** The downhole V_s measurements in SRK (2017a) were processed based on the approach described in Andrus and Stokoe (2000), at selected locations. In general, the V_s -based method, which relies on small-strain stiffness parameters, produced higher CRR values than the other methods that are based on large-strain behavior. For this reason, only the iBPT, SPT/LPT, CPT, and BPT results are presented in the following section.

The factor of safety against liquefaction triggering (FS_{liq}) was computed as the ratio between CRR and CSR, for a reference stress level and earthquake magnitude. A soil exhibiting sand-like behaviour is considered susceptible to liquefaction if FS_{liq} is less than 1.1. If FS_{liq} is greater than 1.1 but less than 1.4, some degree of strength and stiffness degradation is expected.

8.2 Liquefaction Assessment Results

The liquefaction assessment results are presented in Appendix C. Examples of the analysis stages and results for DH19-21 (TP4) are presented in Figure C.1, which includes the following four plots:

- The 11 CSR profiles obtained from the site response analysis, along with the average of all records.
- A penetration resistance profile calculated from the iBPT N_{60} data with correction factors applied to account for stress level and fines content.
- A comparison between the average CSR and the calculated CRR profile (scaled based on a reference stress level and earthquake magnitude). Note that the average CSR is multiplied by the target factor of safety of 1.1 for illustration purposes.
- The resultant FS_{liq} , calculated as the ratio between CRR and CSR.

Plots of the calculated FS_{liq} for the main analysis locations are presented in Figures C.2 to C.8. Results from the iBPT, SPT/LPT, and SCPT data are included where applicable. As noted in Section 8.1.2, the SRK's 2017 BPT data is also included on the plots for comparison purposes.

8.2.1 Tailings Ponds 1 and 2

The liquefaction assessment results for under the crest and downstream toe of Sections A-A' and B-B' are presented on Figure C.2. The plots show that liquefaction may occur in the foundation soils beneath both the crest and toe of TP1 and TP2 to depths of over 30 m. The results appear to be reasonably consistent along the toe of the dam (DH19-02, DH19-04, and DH19-06), with a reducing depth of liquefaction towards the north end of TP1 (DH19-01). The maximum depth of liquefaction under the crest is similar for TP1 and TP2, although the thickness

of the liquefiable layers varies significantly. In general, the depth of liquefaction appears to reduce further away upstream from the crest (DH19-10B and DH19-13).

8.2.2 Tailings Pond 3

Liquefaction assessment results for Sections E-E', F-F', G-G', and I-I' are presented in Figures C.5 to C.8. Based on the available iBPT data, there appears to be limited liquefaction potential in the foundation soils beneath the crest and mid-slope of TP3. At DH19-37B, on the eastern side of TP3 (shown in Figure C.7), the groundwater level is slightly higher than in other areas and FS_{liq} is between 1.1 and 1.4, which indicates that some strength and stiffness degradation is possible.

Across the toe of TP3, the results show reasonably consistent liquefiable layers between El. 1,106 m and 1,085 m (at varying depths from ground surface). In addition, a deeper liquefiable layer is observed at the toe of Section I-I' at around El. 1,070 m (Figure C.8). Towards the southeast corner of TP3, the liquefaction potential appears to reduce significantly, as shown in the second plot on Figure C.8.

8.2.3 Tailings Pond 4

Figures C.3 and C.4 present the results for Sections C-C' and D-D', respectively. Figure C.3 shows that the foundation soils beneath the crest of Section C-C' are not susceptible to liquefaction. This can be attributed to the relatively low predicted CSRs within the foundation soils, due to the significant height of the tailings pond. At the mid-slope location (DH19-42), localized liquefaction is predicted near the groundwater level at El. 1,105 m and within a deeper soil layer between El. 1,085 m and 1,075 m. Extensive liquefaction (depths > 30 m) is predicted under the toe of the dam, based on the iBPT, SPT, and SCPT data.

The results for Section D-D', shown in Figure C.4, appear to be reasonably consistent with those at Section C-C'. Limited liquefaction is predicted under the crest and mid-slope, although some degree of stiffness degradation may occur in localized areas where the FS_{liq} is between 1.1 and 1.4. Extensive liquefaction is again predicted under the dam toe by the iBPT, SPT, and SCPT data. In general, the SRK BPT data does not agree well with the other data sources at these locations.

8.2.4 Tailings Pond 5

The third plot on Figure C.8 presents the results of the liquefaction assessment completed for DH19-28 at the toe of TP5. The results indicate that the foundation soils at the toe are not susceptible to liquefaction, but that softening may occur between El. 1,105 m and 1,100 m, where FS_{liq} is between 1.1 and 1.4. At the crest of TP5, a liquefaction assessment was not completed, since only limited iBPT data was recorded at DH19-40. The geological model shown in Figure 5-9 indicates that the groundwater level is located within the glacial till unit, well below the base of the tailings; therefore, the liquefaction potential beneath the crest of TP5 is not expected to be significant.

8.2.5 Tailings Storage Facility 6

The liquefaction assessment results for several locations at proposed TSF6 are presented on Figures C.9 and C.10. The plots incorporate data from one 2019 iBPT testhole, DH19-57B, along with SPT and SCPT data from the 2012 and 2013 geotechnical investigations in this area. The results from DH19-57B suggest that liquefaction may occur to depths of up to 25 m below ground surface at this location. The historical test data indicates that similar conditions may exist across the site between the river and the base of the slope on the northeast side. Further up the slope, the liquefaction potential appears to be limited based on SPT blow counts and soil descriptions recorded in several boreholes (e.g., GH12-MW07, GH12-MW08, GH12-BH01, GH13-10, and GH13-10).

8.3 Tailings Liquefaction Potential

As shown on the geological cross-sections developed in Section 5.0, the groundwater levels across the TPs were generally found to be close to or below the base of the tailings. In the main liquefaction assessment described in the previous section, the tailings (and other soils) located above the interpreted groundwater level were not considered to be susceptible to liquefaction.

Moisture content measurements and borehole descriptions from the 2019 geotechnical investigation, suggest it is possible that some of the tailings material located above the groundwater level may be poorly drained and exhibit a high degree of saturation.

Published research has shown that as the saturation ratio increases, the resistance against liquefaction or cyclic softening decreases. For example, Grozic et al. (2005) state that as the degree of saturation increased above about 90%, samples began showing a strain-softening behaviour, but samples with lower degrees of saturation strain-hardened. Ishihara et al. (2001) also state that at the saturation ratio of 90%, the cyclic strength becomes 1.8 times as much as that in the case of 100%.

A simplified assessment was carried out to evaluate the liquefaction susceptibility of these tailings with a high saturation ratio. A saturation ratio of 85% was selected as a cut-off where tailings liquefaction behaviour may be observed based on the above studies. The simplified assessment assumed the groundwater table was at the elevation corresponding to 85% saturation ratio. Soils below that elevation were modelled as fully saturated with no increase in their cyclic/liquefaction strength (i.e., zones with saturation ratio of 85% or higher were 100% saturated).

The selection of the 85% threshold and the assumption to ignore the increase in liquefaction strength is considered conservative and was selected with the intent of examining the sensitivity of the model response (seismic deformations) to input parameters.

8.3.1 Tailings Saturation Estimate

An estimate of the degree of saturation of the tailings material in TP1 to TP4 was made based on CPT data from Knight Piesold's 2010 and 2011 investigations, along with moisture content and specific gravity measurements from the 2019 program. The correlation proposed by Robertson and Cabal (2010) was used to calculate unit weight profiles in the tailings for each CPT as a function of the corrected cone resistance, friction ratio, and specific gravity (G_s). In this calculation, $G_s = 2.79$ was used for TP1/TP2 and $G_s = 2.73$ was used for TP3/TP4, based on laboratory tests performed on two tailings samples from the 2019 investigation (BH19-09A-G14 and BH19-35A-G20A). The unit weight profiles and G_s values were then used to estimate the moisture contents required for 85% saturation in the tailings at each location.

On Figure C.11, the measured moisture contents from the 2019 sonic testholes are plotted against the threshold moisture content profiles calculated for each SCPT. It should be noted that the locations of these measurements may not directly correspond to the CPT locations, and the plots are only intended to provide a general comparison for each TP.

The plots show that for TP3 and TP4, the measured moisture contents are generally below the 85% saturation threshold in the upper 20 to 25 m of the tailings, and increase above this threshold closer to the base of the TPs. In TP1 and TP2, there appears to be more scatter in the data, which could be due to higher fines contents in the tailings at these locations. For the purpose of the simplified tailings liquefaction assessment, the elevation at which the tailings saturation may approach or exceed 85% was estimated for each TP, as shown by the dashed lines in Figure C.11. An additional "high estimate" saturation elevation, indicated by the dotted lines, was also used for the FLAC sensitivity analyses discussed in Section 10.0.

8.3.2 Results

The results of the simplified liquefaction assessment for the tailings are presented on Figures C.12 to C.14. The plots indicate that at TP1 and TP2, the tailings below the assumed elevation of 85% saturation may be susceptible to liquefaction, with a FS_{liq} as low as 0.6. At TP3 and TP4, the FS_{liq} in most areas is between 1.1 and 1.4, which suggests that some degree of strength and stiffness degradation may occur; however, at some locations (e.g., DH19-39), liquefaction is possible with a FS_{liq} between 0.9 and 1.1.

The results suggest potential liquefaction in zones near the base of the tailings ponds where higher moisture contents persist. This is not consistent at all locations as it is a function of variable in situ moisture and density conditions. The assessment is based on a limited data set focused around the crests of the tailings pond.

9.0 SLOPE STABILITY ANALYSES

A series of slope stability analyses were performed to evaluate the long-term stability of the tailing ponds, under three design scenarios: static conditions, seismic (pseudo-static) conditions, and post-seismic conditions. The models were based on a combination of collected historical geotechnical investigation data (Table 2-2), the developed geological models (Section 5.0), and the site-specific seismic hazard assessment (Section 7.0). The liquefaction assessment results (Section 8.2) were applied to develop potentially liquefiable material layers in the models.

The following sections describe the methodology, design criteria, models and input parameters, and results of the stability analyses.

9.1 Methodology and Design Criteria

9.1.1 SLOPE/W Software

Limit equilibrium analyses were conducted to determine the factor of safety against slope failure (FS_{slope}) of the existing tailings facilities on site. All analyses were conducted using the commercially available two-dimensional, limit equilibrium software: SLOPE/W (GEO-SLOPE International Ltd., Version 10.0). The Morgenstern-Price method was used throughout the analyses to evaluate potential slip surface failures. Rotational failures were evaluated using the Grid and Radius method and translational failures were evaluated using the Block Specified method. The optimization function was not used for either of these methods.

The principles underlying the method of limit equilibrium for slope stability analyses are as follows:

- A slip mechanism is postulated;
- The shear stresses required to equilibrate the assumed slip mechanism is calculated by means of statics;
- The factor of safety (FS_{slope}) is defined as the ratio of the available shear strength to the calculated shear stresses required for equilibrium; and
- The slip surface with the lowest factor of safety is determined through iteration.

9.1.2 Design Criteria for Factor of Safety against Slope Failure

The CDA guidelines for minimum FS_{slope} values for static, pseudo-static, and post-seismic stability analyses of dams were adopted as noted in Section 6.0.

The selection of a design FS_{slope} for an earth structure (including mining dams) depends on the importance of the structure, potential failure consequences, uncertainties in design loads and soil parameters, and ability to limit the impacts of deformations. The potential failure consequences can vary greatly between shallow and deep slope failures.

For the purpose of this assessment, shallow failures have been defined as slip surfaces contained entirely within the downstream slope of the tailings dams. These types of failures are generally less critical, as they are relatively small with low consequences with respect to public safety and losses towards the economy, environment, and culture. However, shallow failures may develop into more severe problems without maintenance at the time of occurrence. Deep failures were defined as slip surfaces that penetrate through the foundation soils. These are generally larger and more critical failures with higher consequences relating to the above-mentioned items.

The design FS_{slope} values recommended in the CDA guidelines, shown in Table 9-1, were adopted as a starting point for this assessment.

Table 9-1: Factors of Safety Considered in Slope Stability Analyses

Loading Condition	Design Factors of Safety ¹
Static (long-term)	1.5
Seismic (pseudo-static)	1.0
Post-seismic	1.2

¹ Minimum design factors of safety recommended in CDA (2014).

9.2 Stability Analysis Cases and Input Data

9.2.1 Stability Cases Evaluated

The long-term slope stability of the existing tailing ponds was evaluated under several design scenarios:

- Static loading (long-term conditions);
- Seismic (pseudo-static) loading; and
- Post-seismic conditions (static loading with residual undrained shear strength ratios assigned to the materials predicted to experience a reduction in strength).

Seismic loading was modelled using a pseudo-static horizontal PGA of 0.210 g, which corresponds to the 1 in 2,475 years AEP seismic event estimated by the site-specific seismic hazard assessment for the mine site (Section 7.0).

Post-seismic conditions were modelled using residual, undrained shear strength ratios for the materials predicted to liquefy (i.e., $FS_{\text{liq}} < 1.1$) following the design seismic event.

9.2.2 Sections Evaluated

The cross-sections used to develop the slope stability models were selected from the design geological cross-sections presented in Section 5.0 (Figures 5-1 to 5-11). Specifically, each of these geological sections were compared against the other sections with consideration of the sections unique set of parameters, including: locus of boreholes and physical location of data, associated simplified liquefaction triggering assessment results, spatial variation relative to other geological sections, and its physical location relative to site features (i.e., proximity to river, tailing ponds, etc.). As a result, the cross-sections listed below were selected to capture the liquefiable soil conditions across the site based on the distributed parameter variances observed between one geological cross-section to another. The sections selected for the slope stability analyses are listed as follows:

- TP1 – Section A-A’;
- TP2 – Section B-B’;
- TP4 – Sections C-C’ and D-D’; and
- TP3 – Sections F-F’ and G-G’.

Overall, the stability analyses were limited to design sections along TP1 to TP2, and TP3 to TP4. The simplified liquefaction triggering assessment results (Section 8.0) determined that these areas have the largest liquefaction potential. The liquefaction potential within TP5 foundation soils is either not expected to be significant, or the foundation soils were not considered susceptible to liquefaction.

9.2.3 Material Properties

Material properties were selected based on investigation data, correlations with in situ data, and engineering judgement. Material properties used in previous analyses are summarized in Table D (in Tables section) for comparative purposes.

Tetra Tech used various in situ test data to estimate the effective friction angle and residual undrained shear strength ratios of the foundation soils. The iBPT data collected during the 2019 investigation was used as the main data source, since this method provided a continuous profile of penetration resistance versus depth throughout testing operations. Various CPT data was also used during the material parameter review; however, most of the past CPT testing was unable to penetrate through large sections of the existing dam structures and coarse-grained foundation soils.

Drained strength parameters were assigned to all materials in the static and pseudo-static analyses, and to non-liquefiable soil layers in the post-seismic analyses. The effective friction angles were estimated using SPT-based correlations suggested by Schmertmann (1975) and Mayne et al. (2001), and the CPT-based correlations of Kulhawy and Mayne (1990). These correlations provided reasonably comparable results for each location. Due to significant variability in the penetration resistance data across the site, a low estimate friction angle of 34° was conservatively adopted for all foundation soil units, and represents the lower limit of estimated values. This was intended to capture the possibility that loose soil layers within the larger soil units may control the overall stability of the TPs.

Residual undrained shear strength ratios were assigned to liquefiable soils (with $FS_{liq} < 1.1$) in the post-seismic analyses. The residual shear strength ratios were estimated using the SPT and CPT-based correlations proposed by Idriss and Boulanger (2008). The calculated values for soils with a predicted factor of safety against liquefaction of less than 1.1 in the simplified triggering assessment are presented in Figure E.5.

The parameters adopted in the stability analyses for the dam fill materials and foundation soils are summarized in Table 9-2.

Table 9-2: Geotechnical Input Parameters in Slope/W Analyses

Material	Unit Weight, γ (kN/m ³)	Drained Parameters ¹		Undrained Parameters ²
		Effective Friction Angle, ϕ' (°)	Effective Cohesion, c' (kPa)	Liquefied Residual Strength Ratio, S_r/σ'_{vo}
Bedrock (Impenetrable)	-	- ³	-	-
Dam Fill (Waste Rock)	20	39	0	-
Tailings	19	33	0	0.08 ⁴
Glaciofluvial	19	34	0	0.06 – 0.11 ⁵
Colluvium	18	34	0	0.11
Fluvial	18	34	0	0.06 – 0.11 ⁵
Glacial Till	19	34	0	0.09 – 0.11 ⁵

¹ Drained friction angles were used for all materials in the static and seismic (pseudo-static) analyses, and for non-liquefiable materials in the post-seismic analyses.

² Residual undrained shear strength ratios were used for liquefiable soils in the post-seismic analyses.

³ The bedrock is assumed impenetrable and does not have an effective friction angle.

⁴ After EBA 2012

⁵ The residual undrained shear strength ratio was varied depending on the location (i.e., cross-section).

9.2.4 Interpreted Liquefiable Layers

A detailed comparative assessment was conducted at each of the selected design sections (Section 9.2.2) to quantify the configurations of potentially liquefiable layers for the post-seismic slope stability models. All relevant data (i.e., SPT, iBPT, and SCPT data) used in the simplified liquefaction triggering assessment was reviewed and considered in the interpretation of potentially liquefiable layers. The results of this comparative assessment also identified two additional configurations of potentially liquefiable layers to be included as part of the slope stability analyses: Section A-A'₂ and Section B-B'₂.

Figures D.1 and D.2 illustrate tributary areas of data associated with this review at selected sections. These areas demonstrate the broad range of data included in the interpretations for the corresponding section.

Figures D.3 to D.15 present the interpreted liquefiable layers against the results of the simplified liquefaction triggering assessment for each selected section. Figures D.4 and D.6 show two configurations of potentially liquefiable layers used in the analyses along Section A-A' (Section A-A'₂) and Section B-B' (Section B-B'₂). These interpreted liquefiable layers were all directly translated to the according slope stability models for post-seismic analyses.

9.2.5 Sensitivity Analyses

For Sections A-A' and D-D', sensitivity analyses were completed in which the liquefiable layers for the post-seismic cases were defined based on the results of the FLAC deformation analyses presented in Section 10.0 (maximum-intensity earthquake). The FLAC analyses provide contour plots of the maximum excess porewater pressure ratio

($R_{u,max}$) occurring across the soil profile at any point during earthquake shaking. Based on the FLAC output, material strength properties in the Slope/W sensitivity analyses were assigned as follows:

- Soil zones with $0.8 \leq R_{u,max} \leq 1.0$ were assigned undrained liquefied strength ratios consistent with the main Slope/W analyses;
- Soil zones with $0.2 \leq R_{u,max} < 0.8$ were assigned reduced effective friction angles, calculated as a function of $R_{u,max}$; and
- Soil zones with $R_{u,max} < 0.2$ were considered non-liquefiable and assigned their original effective friction angle.

9.3 Stability Analysis Results

Tetra Tech completed the following series of slope stability analyses of the existing tailings pond configurations. Each selected design cross-section was evaluated under static, seismic (pseudo-static), and post-seismic cases, and was compared against the FS_{slope} design criteria presented in Table 9-1.

Table 9-3 presents FS_{slope} results of the stability analyses evaluated under static and seismic conditions. Translational failures were also considered; however, as potentially liquefiable layers are not included in the static and seismic models, FS_{slope} for translational failures were generally higher than the values presented for rotational failures. The FS_{slope} values indicated in red fall below the adopted design criteria for the corresponding design scenario. A summary of results is listed as follows:

- Generally, FS_{slope} for shallow rotational failures (under static and seismic conditions) do not meet the adopted design criteria. These lower FS_{slope} values may be considered acceptable when considering the failure consequence is relatively low and does not represent a threat to the overall structure. If required, the shallow slip surface failures may be addressed by flattening the downstream slope of the tailings dams or as part of post-closure maintenance.
- FS_{slope} for deep rotational failures at Section B-B' (and B-B'₂), Section C-C', Section D-D', and Section F-F' are above or meet the adopted design criteria.
- FS_{slope} for deep rotational failures at Section A-A' (and A-A'₂) and Section G-G fall just below the adopted design criteria.

Slope stability figures for the deep rotational failure results are illustrated in Figures D.16 to D.27 (Appendix D). Section A-A'₂ and Section B-B'₂ are represented by Section A-A' and Section B-B', respectively, in static and seismic conditions as potentially liquefiable layers are not included in these models.

Table 9-3: Summary of Minimum Calculated Factors of Safety for Static and Seismic Scenarios

Tailings Facility	Cross-Section	Design Scenarios				Figures ⁵
		Static ¹		Seismic ² (Pseudo-static)		
		Shallow Rotational Failure ³	Deep Rotational Failure ⁴	Shallow Rotational Failure ³	Deep Rotational Failure ⁴	
TP1	A-A' (A-A' ₂) ⁶	1.05	1.41	0.65	0.95	D.16 D.17
TP2	B-B' (B-B' ₂) ⁶	1.09	1.56	0.73	1.00	D.18 D.19
TP4	C-C'	1.52	1.89	0.95	1.13	D.20 D.21
	D-D'	1.56	1.81	1.00	1.08	D.22 D.23
TP3	F-F'	1.02	1.50	0.67	1.03	D.24 D.25
	G-G'	1.02	1.42	0.94	0.95	D.26 D.27

¹ The adopted minimum $FS_{\text{slope}} = 1.5$ for static conditions.

² The adopted minimum $FS_{\text{slope}} = 1.0$ for seismic (pseudo-static) conditions.

³ Minimum slip surface depth defined at 0.5 m. FS_{slope} for shallow rotational failures penetrate through the surface of the downstream slope of the dam. These failures are typically surface sloughs and do not have critical impact on dam integrity.

⁴ Deep failures defined as slip surfaces that penetrate through the foundation soils.

⁵ Figures in Appendix D present only the deep rotational failures.

⁶ Section A-A'₂ and Section B-B'₂ are represented by the Section A-A' and Section B-B', respectively, in static and seismic conditions as potentially liquefiable layers are not included in these models.

Table 9-4 presents FS_{slope} results of the stability analyses evaluated under post-seismic conditions. Translational failures were considered in post-seismic conditions to account for the possibility of a sliding mechanism developing within a horizontal liquefiable layer. The FS_{slope} values indicated in red fall below the adopted design criteria for the corresponding design scenario. A summary of results is listed as follows:

- FS_{slope} for deep rotational failures of all sections did not meet the adopted design criteria.
- FS_{slope} for translational failures of all sections did not meet the adopted design criteria.
- Sensitivity cases were evaluated for Sections A-A' and D-D' which incorporated the liquefiable layers predicted from the FLAC analyses presented in Section 10. These cases generally show an increase in FS_{slope} values compared to the baseline Slope/W analyses with liquified layers determined with the simplified assessment. This suggests that the simplified liquefaction assessment may lead to a conservative estimate of liquefaction potential compared to the more detailed FLAC analyses.

Slope stability results for the deep rotational failures and translational failures are illustrated in Figures D.28 to D.47 (Appendix D).

Table 9-4: Summary of Minimum Calculated Factors of Safety for Post-Seismic Scenario

Tailings Facility	Cross-Section	Basis of Analysis ¹	Post-seismic ²			Figures ⁵
			Shallow Rotational Failure ³	Deep Rotational Failure ⁴	Translational Failure	
TP1	A-A'	Simplified Liquefaction Assessment	-	0.92	0.83	D.28 D.29
		FLAC Liquefiable Layers	-	1.09	1.05	D.30 D.31
	A-A' ₂	Simplified Liquefaction Assessment	-	0.73	0.66	D.32 D.33
TP2	B-B'	Simplified Liquefaction Assessment	-	0.99	0.72	D.34 D.35
	B-B' ₂	Simplified Liquefaction Assessment	-	0.57	0.20	D.36 D.37
TP4	C-C'	Simplified Liquefaction Assessment	-	0.50	0.17	D.38 D.39
	D-D'	Simplified Liquefaction Assessment	-	0.62	0.14	D.40 D.41
		FLAC Liquefiable Layers	-	0.88	0.85	D.42 D.43
TP3	F-F'	Simplified Liquefaction Assessment	-	0.84	0.78	D.44 D.45
	G-G'	Simplified Liquefaction Assessment	-	0.61	0.15	D.46 D.47

¹ Interpreted liquefiable layers incorporated into the slope stability models were generally based on the simplified liquefaction assessment. Liquefiable layers based on the FLAC analyses were also evaluated, but as sensitivity analyses.

² The adopted minimum $FS_{\text{slope}} = 1.2$ for post-seismic design scenarios.

³ No recorded shallow failures under post-seismic conditions.

⁴ Deep failures defined as slip surfaces that penetrate through the foundation soils.

⁵ Figures in Appendix D present results of deep rotational failures and translational failures.

Overall, the slope stability analyses demonstrate tailings pond instability under post-seismic conditions and require remediation to meet the minimum adopted FS_{slope} . Potential remedial options are briefly discussed in Section 11.0 for further development in the remedial options assessment.

10.0 DEFORMATION ANALYSES

Non-linear effective stress analyses were completed using the computer program FLAC Version 8.0 (Itasca 2016) to estimate the extent of seismic liquefaction and deformation of the tailings ponds. The analyses focused on two cross-sections, Section D-D' (TP4) and Section A-A' (TP1), which were selected as representative examples of the geotechnical conditions and tailings dam geometries in the TP3/TP4 and TP1/TP2 areas. The work consisted of a baseline set of analyses for each section, followed by a detailed sensitivity study to evaluate the potential range of responses across the TPs.

The baseline analyses were undertaken to examine the site-specific response at Sections A-A' and D-D, using representative geotechnical profiles and properties. At each location, the suite of 11 earthquake records was analyzed for the current TPs configuration.

Sensitivity analyses were also carried out to examine the impact of variability and uncertainty in the geotechnical input parameters on the liquefaction extent and TP displacements, and to identify conditions that could lead to an unstable model response. The analyses were conducted using the maximum-intensity earthquake record and are intended to provide an estimate of the range of potential TP displacements.

Deformation analyses figures are presented in Appendix E.

10.1 Methodology

10.1.1 FLAC Software

Dynamic time history analyses were performed using the 2D finite difference software FLAC Version 8.0 (Itasca 2016). The modelling consisted of coupled fluid-mechanical, non-linear effective stress analyses to evaluate the extent of liquefaction and ground deformation induced during earthquake shaking. In these analyses, the PM4SAND constitutive model was used for coarse-grained soil layers to model excess porewater pressure generation during cyclic loading and its impact on soil strength and stiffness.

10.1.2 Geotechnical Parameters and Constitutive Models

The soil profiles and groundwater levels for each cross-section were defined based on the geological model developed in Section 5.0. For the baseline FLAC analyses the main geological units were divided into smaller sub-zones, based on the interpreted geotechnical parameters from the site investigation data (Tetra Tech 2020a). In the sensitivity analysis study, the foundation soils were defined with uniform geotechnical properties, which were varied across a wide range to assess their influence on the model response.

The key geotechnical input parameters used in the FLAC analyses are as follows:

- $(N_1)_{60-cs}$ values for coarse-grained materials were derived primarily from the 2019 iBPT test data, with corrections for stress level and fines content. The site-wide $(N_1)_{60-cs}$ data within the foundation soils and tailings material is summarized in Figures E.1 and E.2. The calculated percentile values (ranging from 5th to 50th) for each TP are also shown on the plots.
- Shear wave velocity (V_s) profiles were obtained from the available SCPT and DST data, and normalized to a reference stress level equal to atmospheric pressure (V_{s1}). Because limited test data was available for the dam fill, the SPT-based correlations for gravelly soils by Rollins et al. (1998) were used to estimate V_{s1} for this material. The site-wide V_{s1} data for the foundation soils and tailings is presented, along with calculated percentile values, in Figures E.3 and E.4.
- Hydraulic conductivities for each layer were estimated as a relative order of magnitude using CPT-based correlations, soil descriptions, and particle size distribution data.
- Post-liquefaction undrained residual shear strengths (S_r) were applied to the liquefied soil zones at the end of earthquake shaking. The residual shear strength ratios (S_r/σ'_v) were calculated as a function of $(N_1)_{60}$ based on correlations proposed by Idriss and Boulanger (2008). Figure E.5 presents the calculated values for soils with a predicted factor of safety against liquefaction (FS_{liq}) of less than 1.1 in the simplified triggering assessment.

Coarse-grained soil layers were modelled with the PM4Sand constitutive model Version 3.1 (Boulanger and Ziotopoulou 2017), which is capable of modelling excess porewater pressure generation during cyclic loading and its impact on soil strength and stiffness. The PM4Sand model parameters were calibrated for each soil unit to achieve a target CRR, using the liquefaction triggering procedure in Boulanger and Idriss (2014). Secondary calibration parameters were also adjusted to match the target stiffness degradation and damping relationships (e.g., Seed and Idriss 1970).

The bedrock unit at the base of the models was defined with elastic parameters. For this layer, the stiffness degradation and damping behaviours were modeled using the built-in 'sig4' hysteretic damping model, which employs a nonlinear backbone curve defined by the Masing rule. The sig4 model was calibrated to replicate the modulus reduction and damping curves of EPRI (1993) for rock.

The hysteretic damping applied in FLAC is generally insufficient to produce adequate damping at small strain levels, so a small amount of Rayleigh damping equal to 0.5% of critical damping at a frequency of 1.5 Hz was applied to all zones in the model.

10.1.3 Input Ground Motions

The 11 crustal ground motion records provided by OSC and used in the FLAC analyses are summarized in Table 7-1. A factor of 0.8 was applied to convert the ground motions from Site Class C (very dense soil or soft rock) to Site Class B (rock). This conversion factor was required because the ground motions were applied within the bedrock unit, which was assigned a typical Site Class B shear wave velocity of 1,100 m/s.

Cumulative Absolute Velocity (CAV) is presented for each of the factored records in Table 10-1 and Figure E.6 as an earthquake intensity parameter. According to the CAV values, the Imperial Valley (IV) record has the maximum intensity and the Sierra Madre (SM) record is representative of the mean intensity which are shown in the table below.

Table 10-1: Calculated Cumulative Absolute Velocities (CAV) for each Earthquake Record

ID	Event	M _w	Station	Duration (s)	CAV ¹ (m/s)
IV	Imperial Valley, 1979	6.5	CPE	64	11.33
CO1	Coalinga, 1983	6.4	PG3	60	3.28
CO2	Coalinga, 1983	6.4	SC3	60	3.97
MH	Morgan Hill, 1984	6.2	CLS	28	3.45
CV	Chalfant Valley, 1986	5.8	BPL	40	4.16
WN	Whittier Narrows, 1987	6.0	SYL	40	5.20
NR1	Northridge, 1994	6.7	CYP	30	4.23
NR2	Northridge, 1994	6.7	UCL	60	6.55
SM	Sierra Madre, 1991	5.6	LAC	65	5.37
NI1	Niigata, Japan, 2004	6.6	FKH21	180	6.10
NI2	Niigata, Japan, 2004	6.6	NIG016	172	6.67
Mean					5.48

¹ Considers the 0.8 factor applied to all records.

10.1.4 Model Configuration and Boundary Conditions

The two-dimensional FLAC models were developed based on the geological cross-sections presented in Section 5.0. For each cross-section, the existing ground surface was defined based on the available survey data, and the base of the model was set at a depth of at least 20 m below the interpreted bedrock surface. To reduce boundary effects, the lateral boundaries were set a minimum distance of 150 m to 200 m away from either side of crest and the toe of the TP dam.

During the initialization stages, the model was brought to mechanical and groundwater flow equilibrium. Initial static equilibrium was achieved by using the linear elastic material model, which was then replaced by the Mohr-Coulomb model, followed by the PM4Sand model in applicable zones. At the start of the dynamic analyses, the model displacements were reset to zero; Rayleigh and hysteretic damping were activated in the relevant zones; and groundwater flow was enabled. The lateral edges of the model were defined as free-field (energy absorbing) boundaries, and the base of the model was defined as a quiet boundary to simulate non-reflecting and energy-absorbing boundary conditions. The input earthquake motions were applied to the quiet base boundary as shear stress-time histories, calculated using the incident velocity-time histories from the selected ground motion records.

At the end of earthquake shaking, a post-seismic deformation analysis step was performed. In this step, the soil zones considered to have liquefied (with a maximum excess porewater pressure ratio greater than 0.7) were assigned the Mohr-Coulomb material model and a post-liquefaction undrained residual shear strength based on $(N_1)_{60}$ correlations. In addition, soil zones exhibiting dilation (negative excess porewater pressures) at the end of shaking were assigned undrained shear strengths equal to the initial drained strength. The lateral and base boundaries were then fixed, and the model was allowed to deform under the adjusted strength conditions until equilibrium was reached.

10.1.5 Output

At the end of the FLAC analyses, the following data were extracted from the models:

- Maximum excess porewater pressure ratio, $R_{u,max}$, in each zone at the end of shaking;
- Horizontal and vertical slope displacements at the end of shaking; and
- Horizontal and vertical slope displacements at the end of the post-seismic deformation step.

The output data provides an indication of the extent of liquefaction and the magnitude of seismic ground displacements during and shortly after shaking (also referred to as shear-induced displacements) at each cross-section.

The FLAC displacement values do not include further post-seismic volumetric deformations that are expected to occur as excess porewater pressures dissipate and liquefied materials re-consolidate and settle. Post-seismic volumetric settlements were estimated using the methods of Tokimatsu and Seed (1987) and Wu (2002) for coarse-grained soils.

10.2 TP4 – Section D-D'

10.2.1 Section D-D' Input Parameters

The FLAC model used for the baseline analyses of Section D-D' is shown in Figure E.7.

The geotechnical input parameters used in the baseline FLAC analysis of Section D-D' are summarized in Table 10-2. In Figures E.8 and E.9, the selected design profiles for $(N_1)_{60-cs}$ and V_{s1} are plotted against the test data obtained at the crest, mid-slope, and toe of TP4. Based on the recommendations in Montgomery and Boulanger (2016), 33rd percentile $(N_1)_{60-cs}$ values from the testholes nearest to the cross-section were used for each soil layer. In addition, a pessimistic soil profile for TP4, shown by the red dotted line, was considered in the sensitivity study. For the V_{s1} parameter, average values were selected for each layer based on the relevant nearby testholes.

Table 10-2: Key Geotechnical Input Parameters for Section D-D' Baseline Analyses

Unit	Layer ID	Unit Weight (kN/m ³)	$(N_1)_{60-cs}$	V_{s1} (m/s)	V_s (m/s)	Hydraulic Conductivity ¹ (m/s)	Constitutive Model
Tailings	Tailings_17	19	17	215	-	5.0E-06	PM4SAND
	Tailings_11	19	11	175	-	5.0E-07	
Dam Fill	Fill	20	25	240	-	1.0E-04	
Fluvial	FL	18	18	260	-	5.0E-05	
Glaciofluvial	GF_15	19	15	310	-	5.0E-05	
	GF_20	19	20	310	-	5.0E-05 (Upper) 1.0E-05 (Lower)	
	GF_10	19	10	310	-	5.0E-07 (Crest) 1.0E-05 (Toe)	
	GF_23	19	23	310	-	1.0E-05	
	GF_27	19	27	310	-	1.0E-05	
	GF_14	19	14	310	-	1.0E-05	
	GF_30	19	30	350	-	1.0E-06	
	GF_8	19	8	250	-	5.0E-07	
Bedrock	Bedrock	22	-	-	1,100	1.0E-08	Elastic – Hysteretic

¹ Vertical hydraulic conductivity was taken as ½ of the horizontal value.

10.2.2 Section D-D' Baseline Analyses

Figure E.10 presents a contour plot of $R_{u,max}$ for the maximum-intensity record (IV) at the end of earthquake shaking. The plot shows extensive liquefaction, indicated by $R_{u,max}$ values of up to 1.0, between the dam toe and the Flat River. A smaller region of elevated $R_{u,max}$ values is observed underneath the tailings, while very limited excess porewater pressures appear to develop under the dam. In general, the overall extent of liquefaction is greater under the maximum-intensity earthquake compared to the other records analyzed. The excess porewater pressure distribution appears to be reasonably consistent with the results of the simplified liquefaction assessment, with deep liquefiable layers predicted to around El. 1,080 m near the dam toe.

Contour plots of shear-induced displacements and maximum shear strains at the end of earthquake shaking are presented for the IV record in Figure E.11. The displacement contours show horizontal displacements occurring on

both sides of the model toward the Flat River, along with settlement of the TP4 dam crest and heave of the riverbed. The most significant horizontal displacements tend to occur on the opposite side of the river from TP4; this is due to the greater extent of liquefaction in this area, which allows a sliding mechanism to develop. On the TP4 dam, localized areas of larger displacements occur at the crest (0.44 m) and toe (0.30 m), while global slope displacements are relatively smaller.

A comparison of the horizontal displacement contours at the end of shaking and after the post-seismic analysis step is provided for the IV record in Figure E.12. The plots show that localized displacements at the dam toe increase after the post-seismic step to 0.47 m, while the displacements at the crest are not noticeably affected. On the opposite side of the river, the displacements increase significantly after the post-seismic step due to the extensive liquefaction observed in this area.

The seismic displacements at the ground surface of the TP4 crest, mid-slope, and toe are plotted against the CAV parameter for each earthquake record in Figures E.13a and E.13b. Figure E.13a presents the displacements extracted from the FLAC model at the end of shaking, while the first two plots in Figure E.13b show the FLAC displacements after the post-seismic analysis step. The third plot in Figure E.13b shows the total post-seismic vertical displacements, which combine the FLAC results and the estimated post-liquefaction volumetric settlement. The predicted volumetric settlements tend to be largest near the dam toe (up to 0.65 m), where higher excess porewater pressures are observed in the FLAC analyses. The plots all show a general increase in the magnitude of displacement with increasing CAV.

10.2.2.1 Summary

The post-seismic horizontal and vertical displacements at the dam crest and toe of Section D-D' are summarized in Table 10-3 (maximum-intensity record) and Table 10-4 (average of 11 records).

Table 10-3: Post-Seismic Displacements – Section D-D' Baseline Analyses (Maximum-Intensity Earthquake Record)

Analysis Case	Horizontal Displacement – IV Record (m)		Vertical Displacement ¹ – IV Record (m)	
	Crest	Toe	Crest	Toe
Baseline	0.44	0.47	-0.21	-0.65

Table 10-4: Post-Seismic Displacements – Section D-D' Baseline Analyses (Average of 11 Earthquake Records)

Analysis Case	Average Horizontal Displacement (m)		Average Vertical Displacement ¹ (m)	
	Crest	Toe	Crest	Toe
Baseline	0.17	0.12	-0.09	-0.13

¹ Total including FLAC displacements and estimated post-seismic volumetric displacements. Negative values indicate settlement.

10.2.3 Section D-D' Sensitivity Analyses

Sensitivity analyses were undertaken using the maximum-intensity earthquake record (IV) to assess the impact of variability and uncertainty in the geotechnical parameters on the liquefaction extent and TP displacements. The foundation soils were defined with uniform geotechnical properties and the following parameters were varied across a relatively wide range: $(N_1)_{60-cs}$ (penetration resistance), V_{s1} (initial soil stiffness), and k (hydraulic conductivity). The liquefaction potential of the tailings material was also assessed by increasing the groundwater level upstream of the dam to the best and highest estimate elevations for 85% tailings saturation, as defined in Section 8.3. An additional analysis using a pessimistic soil profile, defined in Figure E.8, was carried out for comparison with the baseline case.

The analysis cases and range of parameters assessed are summarized in Table 10-5. FLAC output plots for selected analyses are shown in Figures E.14 to E.19, and a summary of the horizontal displacements for all sensitivity cases is provided in Figures E.20.

Table 10-5: Section D-D' Sensitivity Analysis Cases

Analysis Case	Parameters Evaluated ¹			
	$(N_1)_{60-cs}$	V_{s1} (m/s)	Hydraulic Conductivity ² , k (m/s)	Groundwater Elevation ³ , GWL (m)
$(N_1)_{60-cs}$	5, 10, 15, 20	310	1.0E-5	1110
V_{s1}	10	200, 400	1.0E-5	1110
k	10	310	1.0E-6, 1.0E-4	1110
GWL	10	310	1.0E-5	1120, 1125, 1130
Pessimistic	Pessimistic Profile	Baseline Profile	Baseline Profile	1110 (Baseline)

¹ Parameters applied to the foundation soils only. Baseline parameters are applied to tailings, dam, and bedrock layers.

² Vertical hydraulic conductivity was taken as $\frac{1}{2}$ of the horizontal value.

³ Refers to the approximate elevation of the groundwater immediately upstream of the dam. The approximate elevation of the base of the tailings is 1111 m at this location.

Contour plots of $R_{u,max}$ and horizontal displacement at the end of shaking are shown for the $(N_1)_{60-cs}$ analysis case in Figures E.14 and E.15. Figure E.14 shows that a reduction in the $(N_1)_{60-cs}$ parameter leads to an increase in excess porewater pressures in the foundation soils beneath the TP. When $(N_1)_{60-cs}$ is reduced to a uniform value of 5, a continuous layer of high excess porewater pressures develops beneath the slope and the displacements increase by several meters, as shown in Figures E.15a and E.15b.

The results of the tailings groundwater level assessment are shown in Figures E.16 and E.17. The plots show that the elevated groundwater level leads to a minor increase in $R_{u,max}$ within the tailings, which is consistent with expectations based on the simplified tailings liquefaction assessment presented in Section 8.3. The higher groundwater levels are also associated with a slight increase in displacement at the end of shaking, over a larger area of the slope, as shown in Figure E.17. In general, this parameter does not appear to have as significant impact as the $(N_1)_{60-cs}$ value used in the foundation soils.

The $R_{u,max}$ and horizontal displacement contours for the pessimistic soil profile are compared to the baseline results in Figures E.18 and E.19. In the pessimistic case, continuous elevated excess porewater pressures develop beneath the slope in a lower layer with $(N_1)_{60-cs} = 5$, which causes an increase in both the magnitude of the horizontal displacements and the area of the slope that is affected, compared to the baseline case.

The horizontal displacements for the current configuration of Section D-D' are summarized in Figures E.20a (end of shaking) and E.20b (post-seismic). In these figures, the crest and toe displacements from the four parametric cases are plotted against $(N_1)_{60-cs}$, and compared with the pessimistic and baseline results, which are shown as horizontal lines. The 5th, 10th, and 33rd percentile $(N_1)_{60-cs}$ values calculated for TP4 are also included on the plots for reference.

The plots show that $(N_1)_{60-cs}$ has the largest impact on the horizontal displacements over the range of parameters examined. The displacements tend to increase dramatically when $(N_1)_{60-cs}$ is reduced to 5; however, it should be noted that this is an unrealistically low value when applied uniformly to the foundation soils, given the percentiles calculated from the iBPT data. In the baseline analysis case, the displacements at the TP crest and toe are generally in line with the sensitivity results for $(N_1)_{60-cs} = 15$, which is close to the 33rd percentile value calculated for TP4. In the pessimistic case, the displacements are closer to the results for $(N_1)_{60-cs} = 10$.

The post-seismic displacements for the pessimistic analysis case under the maximum-intensity earthquake are compared to the baseline analysis results in Table 10-6.

Table 10-6: Post-Seismic Displacements – Section D-D' Pessimistic vs. Baseline Analyses (Maximum-Intensity Earthquake Record)

Analysis Case	Horizontal Displacement – IV Record (m)		Vertical Displacement ¹ – IV Record (m)	
	Crest	Toe	Crest	Toe
Pessimistic	0.76	0.93	-0.55	-0.24
Baseline	0.44	0.47	-0.21	-0.65

¹ Total including FLAC displacements and estimated post-seismic volumetric displacements. Negative values indicate settlement.

10.2.4 Section D-D' Discussion

The baseline analyses for Section D-D' show that significant liquefaction may occur beyond the toe of the dam, and elevated excess porewater pressures may develop beneath the dam crest and tailings. Between the dam toe and crest, excess porewater pressures in the foundation soils tend to decrease abruptly. The FLAC results indicate reduced extent of liquefaction beneath the dam footprint compared to the extent considered in the post-seismic Slope/W analyses, which was based on the simplified liquefaction triggering assessment.

The reduction in excess porewater pressures directly beneath the dam is likely due to initial static shear stresses within the slope, which may reduce the liquefaction susceptibility of the foundation soils compared to free-field conditions, due to the tendency of the soil elements to dilate given their initial density. The sensitivity analyses showed that the relative density of the foundation soil unit would have to be reduced to an unrealistically low value, $(N_1)_{60-cs} = 5$, for a continuous layer of high excess porewater pressures to develop beneath the slope, which in turn leads to a significant increase in the slope displacements.

The sensitivity analyses were intended to provide an indication, using the maximum-intensity earthquake record, of the potential range of horizontal displacements that could occur under varying foundation conditions. Based on a review of the in situ geotechnical test data for TP4, the baseline analyses are considered to provide a best estimate of the deformation response at Section D-D' (Tables 10-3 and 10-4), while the pessimistic analysis case provides a high estimate of the displacements at TP4 (Table 10-6).

Given the magnitude of displacements predicted in these analyses (up to 1 m in the pessimistic case), and the low groundwater levels measured within the tailings, it appears that a breach-type failure of TP4 is not likely to occur under the design seismic loads. However, further analysis such as a dam breach assessment with consideration of multiple failure modes would be required to evaluate the risks and potential consequences of a breaching failure.

Although FLAC analyses were not conducted for specific cross-sections through TP3 due to the similar geotechnical conditions observed in this area, the TP3 displacements are expected to be within the same general range as those predicted for TP4. Additional analyses to confirm TP3 displacements are recommended as part of the detailed design stage.

10.3 TP1 – Section A-A'

10.3.1 Section A-A' Input Parameters

The FLAC model used for the baseline analyses of Section A-A' is shown on Figure E.21.

The geotechnical input parameters used in the baseline FLAC analysis of Section A-A' are summarized in Table 10-7. In Figures E.22 and E.23, the selected design profiles for $(N_1)_{60-cs}$ and V_{s1} are plotted against the test data obtained at the crest and toe of TP1 and TP2. Using the same approach as for Section D-D', the 33rd percentile $(N_1)_{60-cs}$ values from the testholes nearest to Section A-A' were selected for each soil layer, and average values were selected for the V_{s1} parameter. Additionally, a pessimistic soil profile for TP1/TP2, shown by the red dotted line, was considered in the sensitivity analyses.

Table 10-7: Key Geotechnical Input Parameters for Section A-A' Baseline Analyses

Unit	Layer ID	Unit Weight (kN/m ³)	$(N_1)_{60-cs}$	V_{s1} (m/s)	V_s (m/s)	Hydraulic Conductivity ¹ (m/s)	Constitutive Model
Tailings	Tailings	19	18	230	-	5.0E-07	PM4SAND
Dam Fill	Fill	20	25	240	-	1.0E-04	
Fluvial	FL	18	20	330	-	5.0E-06	
Colluvium	CL_30	18	30	260	-	5.0E-06	
	CL_16	18	16	260	-	5.0E-06	
Glaciofluvial	GF_20	19	20	330	-	5.0E-05	
	GF_14	19	14	330	-	5.0E-05	
	GF_22	19	22	330	-	5.0E-05	
	GF_5	19	5	330	-	5.0E-05	
	GF_13	19	13	330	-	1.0E-05	
	GF_29	19	29	330	-	5.0E-06	
Bedrock	Bedrock	22	-	-	1,100	1.0E-08	Elastic – Hysteretic

¹ Vertical hydraulic conductivity was taken as ½ of the horizontal value.

10.3.2 Section A-A' Baseline Analyses

Figure E.24 presents a contour plot of $R_{u,max}$ for Section A-A' under the maximum-intensity record (IV). The plot shows that significant liquefaction occurs beneath the tailings and beyond the toe of the dam, which is consistent with the results of the simplified triggering assessment. Directly beneath the dam slope, the $R_{u,max}$ values reduce to a maximum of around 0.6. As noted in the Section D-D' discussion, this reduction is likely due to initial static shear stresses in the foundation soils beneath the slope, which may decrease the liquefaction susceptibility compared to free-field conditions.

Contour plots of shear-induced displacement and maximum shear strains at the end of earthquake shaking are presented for the IV record in Figure E.25. The plots show that horizontal slope displacements occur in the direction of the Flat River, along with minor settlement of the TP crest and heave at the TP toe. The displacements appear to be associated with a global sliding mechanism along the liquefied layer beneath the TP. After the post-seismic analysis step, the horizontal displacements increase in certain areas along the slope and beyond the dam toe towards the river, as shown in Figure E.26.

The seismic displacements at the ground surface of the TP1 crest, mid-slope, and toe are plotted against the CAV parameter for each earthquake record in Figures E.27a (end of shaking) and E.27b (after the post-seismic step). The figures show that the horizontal displacements generally increase with CAV, while the vertical displacements are relatively similar for different earthquake records. The predicted volumetric settlements, included on the third plot in Figure E.27b, tend to be largest near the dam crest, where a relatively thick liquefiable layer is observed.

The post-seismic horizontal and vertical displacements along Section A-A' at the dam crest and toe are summarized in Table 10-8 (maximum-intensity record) and Table 10-9 (average of 11 records).

Table 10-8: Post-Seismic Displacements – Section A-A' Baseline Analyses (Maximum-Intensity Earthquake Record)

Analysis Case	Horizontal Displacement – IV Record (m)		Vertical Displacement ¹ – IV Record (m)	
	Crest	Toe	Crest	Toe
Baseline	0.52	0.49	-0.58	0.02

Table 10-9: Post-Seismic Displacements – Section A-A' Baseline Analyses (Average of 11 Earthquake Records)

Analysis Case	Average Horizontal Displacement (m)		Average Vertical Displacement ¹ (m)	
	Crest	Toe	Crest	Toe
Baseline	0.24	0.22	-0.47	0.00

¹ Total including FLAC displacements and estimated post-seismic volumetric displacements. Negative values indicate settlement.

10.3.3 Section A-A' Sensitivity Analyses

Sensitivity analyses were undertaken for Section A-A' using the maximum-intensity earthquake record (IV). The same approach adopted for Section D-D' was used to assess the impact of penetration resistance, initial soil stiffness, hydraulic conductivity, and elevated groundwater levels on the Section A-A' model response. In addition,

the pessimistic soil profile defined for TP1 and TP2 in Figure E.22 was analyzed for comparison with the baseline model.

The analysis cases and range of parameters assessed are summarized in Table 10-10. FLAC output plots for selected cases are shown in Figures E.28 to E.33, and a summary of the horizontal displacements for all Section A-A' sensitivity analyses is provided in Figure E.34.

Table 10-10: Section A-A' Sensitivity Analysis Cases

Analysis Case	Parameters Evaluated ¹			
	(N ₁) _{60-cs}	V _{s1} (m/s)	Hydraulic Conductivity ² , k (m/s)	Groundwater Elevation ³ , GWL (m)
(N ₁) _{60-cs}	5, 10, 15, 20	330	1.0E-5	1110
V _{s1}	10	200, 400	1.0E-5	1110
k	10	330	1.0E-6, 1.0E-4	1110
GWL	10	330	1.0E-5	1117, 1121
Pessimistic	Pessimistic Profile	Baseline Profile	Baseline Profile	1110 (Baseline)
Baseline	Baseline Profile	Baseline Profile	Baseline Profile	1110 (Baseline)

¹ Parameters applied to the foundation soils only. Baseline parameters are applied to tailings, dam, and bedrock layers.

² Vertical hydraulic conductivity was taken as ½ of the horizontal value.

³ Refers to the approximate elevation of the groundwater immediately upstream of the dam. The approximate elevation of the base of the tailings is 1112 m at this location.

Contour plots of Ru,max and horizontal displacement at the end of shaking are shown for each (N₁)_{60-cs} case in Figures E.28 and E.29. The plots show that a reduction in the (N₁)_{60-cs} parameter causes an increase in Ru,max values across the model, as well as an increase in the thickness/depth of layers experiencing liquefaction (i.e., Ru,max > 0.7), which in turn leads to larger global slope displacements.

Figures E.30 and E.31 show that increasing the groundwater level results in liquefaction of the saturated tailings at some distance back from the TP crest, which is consistent with the results of the simplified tailings liquefaction assessment. A slight decrease in Ru,max values is also observed beneath the slope, which may be due to the change in stress conditions caused by the increased groundwater level. The overall impact of the higher groundwater levels is a relatively minor increase in the magnitude of the TP dam displacements.

The Ru,max and horizontal displacement contours for the pessimistic soil profile are compared to the baseline results in Figures E.32 and E.33. In the pessimistic case, higher excess porewater pressures develop beneath the slope and at the toe of the dam, which causes an increase in both the magnitude of the horizontal displacements and the area of the TP that is affected, compared to the baseline case.

The horizontal displacement results for the current configuration of Section A-A' are plotted against (N₁)_{60-cs} in Figures E.34a (end of shaking) and E.34b (post-seismic), along with the calculated percentile values for TP1 and TP2. As observed for Section D-D', the (N₁)_{60-cs} parameter appears to have the largest impact on the TP displacements. For the baseline analysis case, the horizontal displacements at the TP crest and toe fall between the sensitivity results for (N₁)_{60-cs} values of 10 and 15. In the pessimistic case, the displacements approach the results for (N₁)_{60-cs} = 5.

The post-seismic displacements for the pessimistic analyses under the maximum-intensity earthquake are compared to the baseline results in Table 10-11.

Table 10-11: Post-Seismic Displacements – Section A-A' Pessimistic vs. Baseline Analyses (Maximum-Intensity Earthquake Record)

Analysis Case	Horizontal Displacement – IV Record (m)		Vertical Displacement ¹ – IV Record (m)	
	Crest	Toe	Crest	Toe
Pessimistic	0.99	1.04	-0.23	-0.19
Baseline	0.52	0.49	-0.58	0.02

¹ Total including FLAC displacements and estimated post-seismic volumetric displacements. Negative values indicate settlement.

10.3.4 Section A-A' Discussion

The baseline analyses of Section A-A' indicate that significant liquefaction of the foundation soils may occur beneath the tailings and at the toe of the TP dam. The results are reasonably consistent with the simplified triggering assessment and the liquefaction extent considered in the post-seismic Slope/W analyses. In the Section A-A' FLAC models, the excess porewater pressures tend to reduce directly beneath the dam slope, but the reduction is generally smaller than seen in the Section D-D' analyses, due to the different material properties and stress conditions in this cross-section. As observed for Section D-D', when the relative density of the foundation soil unit was reduced to $(N_1)_{60-cs} = 5$ in the sensitivity analyses, a more continuous layer of elevated excess porewater pressures developed and the global slope displacements increased.

The baseline results reported in Tables 10-8 and 10-9 are considered a best estimate of the TP1 displacements at Section A-A'. The pessimistic analyses, which consider low estimate $(N_1)_{60-cs}$ values along with the maximum-intensity earthquake record, are intended to provide a high estimate of the displacements across TP1 and TP2 (Table 10-11).

The results suggest that global displacements of the TP may occur in the direction of the Flat River, but a breach-type failure of TP1 or TP2 appears unlikely given the displacement magnitudes (approximately 1 m in the pessimistic model) and the relatively low groundwater levels. However, further analysis such as a dam breach assessment with consideration of multiple failure modes would be required to evaluate the risks and potential consequences of a breaching failure.

11.0 SUMMARY

Geotechnical Site Data

Multiple geotechnical site investigations have been completed at the Cantung Mine site since the mid 1970s to evaluate foundation soils, groundwater conditions, dam composition, borrow sources, and tailings properties. These investigations have been completed within and around the existing tailings pond footprints and at potential new tailings storage locations.

In total, 17 investigations have been completed using various drilling methods including Becker hammer (instrumented and non-instrumented), air rotary, ODEX tricone, mechanical excavation, and sonic drilling. Cone penetration testing (CPT) was completed concurrently with several investigations, providing continuous material

properties (strength and moisture content) through the soil profile. Standard penetration testing (SPT), Becker penetration testing, and large penetration testing also provided soil strength information at discrete locations throughout the soil profile. The most recent investigation was completed by Tetra Tech in 2019 to characterize foundation soils and fill in gaps or uncertainties identified in previous investigation results.

Geological Model

Tetra Tech developed a geological model of the tailings ponds (foundation conditions and superstructure) by integrating data from the geotechnical investigations, historical air photos, pre-development terrain mapping, and design and construction record reports. Interpretation of the data was often required when comparing multiple sources as a better understanding of the local stratigraphy and depositional history was formed. A site-specific seismic hazard assessment was also completed to determine the design earthquake loading specific to the Cantung Mine site in closure, passive care conditions.

The liquefaction potential of the tailings dams and foundation soils was evaluated based on the site model, geotechnical investigation results, and the seismic hazard assessment. The liquefaction triggering assessment was undertaken following the approach outlined by Boulanger and Idriss (2014). Preliminary assessment of the liquefaction potential of the impounded tailings was also completed; however, the primary focus of the analyses was on the granular fill of the dams and underlying foundation material.

The tailings ponds are generally located on glaciofluvial and fluvial valley infill, with some colluvium sourced from the valley side slopes. Bedrock under the dam structures is deep (>30 m) and groundwater is at least 2 m below the original ground elevation and base of the tailings ponds, typically following the original ground contours.

The mine site is situated in an area of extensive discontinuous permafrost, which is defined as regions with approximately 50% to 90% of land underlain by permafrost (Natural Resources Canada 1995). Previous investigations have identified some pockets of permafrost at the site; however, these are generally isolated areas and the site can largely be assumed to be underlain by unfrozen ground conditions.

The containment dams are constructed of local glaciofluvial and fluvial materials consisting of a mixture of silts, sands, and gravels, with occasional cobbles and boulders. As-built records show they were constructed in stages using upstream, downstream, and centerline methods, to provide tailings containment capacity. Tailings have typically been deposited subaerially around the pond perimeter resulting in segregated beach deposits. Limited segregated tailing placement (from cyclone processing) also occurred during underground backfill operations.

Liquefiable soils were identified under TP1 through TP4 and are generally located in the glaciofluvial and colluvium soils. Post-seismic softening of the foundation soils were predicted under TP5; however, liquefaction of the foundation soil is not expected. Liquefiable soils extend under the crest and toe of TP1 and TP2, but are generally isolated to the toe of TP3. Liquefiable soils were identified under the toe of TP4 and to a limited extent under the mid-slope.

The tailings themselves show a varying response to seismic loading. In the upper portion of the tailings ponds, the tailings are largely unsaturated and are generally not susceptible to liquefaction during seismic loading. Moisture contents increase toward the base of the deposits, nearing saturated conditions at depth. Analysis shows a potential for basal tailings liquefaction in TP1 and TP2, and some degree of softening in TP3 and TP4; however, the dam embankments are not susceptible to liquefaction.

Geotechnical data is largely concentrated inside or within close proximity to the dam footprints. The data density upstream of the dams, within the impounded tailings themselves, is more dispersed requiring increased interpretation of soil stratigraphy between data points. The current model is considered adequate for concept level

analysis and design; however, additional site data may be required, particularly from within the tailings pond footprint.

The Cantung tailings dams are currently classified as having a Significant consequence of failure based on CDA guidelines and have been analyzed accordingly.

Geotechnical Analysis

Stability analyses indicate the current tailings pond configurations generally meet CDA criteria under static and pseudo-static loading conditions. Some shallow sloughing of the downstream slope may occur during large runoff or small earthquake events; however, these shallow failures will not affect the overall integrity of the dam. If required, the shallow slip surface failures may be addressed by flattening the downstream slope of the tailings dams or completing maintenance following a destabilizing event.

The current tailings pond configurations showed instability under the post-seismic condition, with the failure mode predominantly driven by translational failure mechanisms.

FLAC analyses for TP1 indicate post-seismic global displacements may occur in the direction of the Flat River, but a breach-type (deep) failure appears unlikely given the displacement magnitudes (approximately 1 m in the pessimistic model) and the relatively low groundwater levels. Similar geotechnical conditions are expected in TP2 and displacements are expected to be within the same general range as those predicted for TP1.

Similarly, FLAC analysis for TP4 show predicted displacements of up to 1 m, assuming pessimistic soils conditions. Given the low groundwater levels measured within the tailings, it appears that a breach-type failure of TP4 is also not likely under the design seismic loads. Similar geotechnical conditions are expected in TP3 and displacements are expected to be within the same general range as those predicted for TP4.

Though breach-type failures are considered unlikely, further analysis such as a dam breach assessment with consideration of multiple failure modes would be required to fully evaluate the risks and potential consequences of a breaching failure.

Stability analyses were completed using liquefiable layers developed from the simplified triggering assessment and the FLAC modelling. The results showed reasonable similarity and provide confidence in the simplified liquefaction assessment approach and its adequacy at this level of analysis. Stability analysis using the simplified assessment typically yielded somewhat lower factors of safety suggesting there may be some conservatism in the reported values.

Long-Term Performance and Remediation

Overall, the dams are considered to be stable under static loading conditions, with the exception of potential shallow downstream slumping or sloughing. Seismic events would initiate slope deformation and movement; however, the risk of massive slope failure and tailings run out is considered low.

Addressing the potential instability observed during post-seismic loading can be broadly approached by either maintaining the existing condition, implementing in situ engineering measures, or removing material overlying potentially liquefiable soils. Possible options under consideration are summarized below and further developed in the ROA:

- **Maintain existing geotechnical condition:** The existing tailings dam slope geometry could be maintained and monitored for acceptable performance. This approach would require a risk assessment that considers the likelihood and consequence of a breaching type failure.

- **Ground improvement:** Ground improvement techniques such as stone columns or jet grouting could be used to provide additional stability at the dam toe during an earthquake event.
- **Stabilization buttress:** A downstream buttress could be constructed to improve post-seismic stability and reduce deformations.
- **Complete tailings excavation:** Tailings and the containment dam could be excavated in their entirety. Tailings could be dry stacked at a facility with foundation soils not susceptible to post-seismic liquefaction. Dam material could then be used as borrow material for site reclamation activities.
- **Partial tailings excavation:** This option is similar to the complete tailings excavation except that excavation would be limited to the area underlain by, and close to, liquefiable soils.

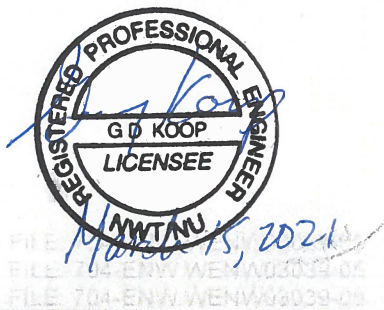
12.0 CLOSURE

We trust this document meets your present requirements. If you have any questions or comments, please contact the undersigned.

Respectfully submitted,
Tetra Tech Canada Inc.

Prepared by:
Chantal Pawlychka, B.Sc., P.Eng.
Geotechnical Engineer, Arctic Region
Direct Line: 587.460.3593
chantal.pawlychka@tetrattech.com

Prepared by:
Elizabeth Williams, DPhil., P.Eng.
Geotechnical Engineer, Pacific Region
Direct Line: 604.608.8643
elizabeth.williams@tetrattech.com



Prepared / Reviewed by:
Gary Koop, M.Eng., P.Eng.
Principal Consultant, Arctic Region
Direct Line: 587.460.3542
gary.koop@tetrattech.com



Reviewed by:
Ali Azizian, Ph.D., P.Eng., PMP
Principal Specialist – Geotechnical / Seismic
Direct Line: 778.945.5733
ali.azizian@tetrattech.com

Reviewed by:
Bob Patrick, M.Sc., P.Eng.
Director, Dam Engineering
bob.patrick@tetrattech.com

/jf

PERMIT TO PRACTICE TETRA TECH CANADA INC.	
Signature	<u>Gary Koop</u>
Date	<u>March 15, 2021</u>
PERMIT NUMBER: P 018	
NT/NU Association of Professional Engineers and Geoscientists	

REFERENCES

- Andrus, R.D. and Stokoe II, K.H. 2000. Liquefaction Resistance of Soils from Shear-wave Velocity. *Journal of Geotechnical and Geoenvironmental Engineering*, 126(11), 1015-1025.
- Boulanger, R.W. and Idriss, I.M. 2014. CPT and SPT Based Liquefaction Triggering Procedure. Report No. UCD/GCM -14/01. Department of Civil & Environmental Engineering, University of California at Davis.
- Boulanger, R.W. and Ziotopoulou, K. (2017). PM4Sand (Version 3.1): A Sand Plasticity Model for Earthquake Engineering Applications. Report No. UCD/CGM-17/01. University of California at Davis, October 2017 (Revised July 2018).
- BGC Engineering Inc. (BGC). 2017 Geomorphological Interpretation, Cantung Mine Reported in SRK, 2017. Assessment of Liquefaction Potential, Dam Stability and Remedial Options for the Tailings Facilities, Cantung Mine, Northwest Territories Geomorphological Interpretation, Cantung Mine. Prepared for North American Tungsten Corporation Ltd., Vancouver, BC. July 2017.
- Canadian Dam Association (CDA). 2013. Dam Safety Guidelines 2007 (2013 Edition).
- Canadian Dam Association (CDA). 2014. Technical Bulletin: Application of 2007 Dam Safety Guidelines to Mining Dams.
- Consolidated Geotechnical Services Inc.(Consol), 1986a. Report to Canada Tungsten Mining Corporation on Tailing Disposal and Reclamation. Submitted to Canada Tungsten Mining Corporation, March 1986. File No.: 86105.
- Consol. 1986b. Dam Construction, Tailings Pond No.5. Letter to Canada Tungsten Mining Corporation, August 18, 1986.
- Department of Energy, Mines and Resources Canada. 1995. Permafrost. The National Atlas of Canada. Natural Resources Canada. Map MCR 4177, Edition 5. Scale 1:7,500,000.
- Dyke, A.S. 1990. Surficial Materials and Landforms, Little Hyland River, Yukon Territory and Northwest Territories. Geological Survey of Canada. Map 1677A. Scale 1:100,000.
- Ecosystem Classification Group. 2010. Ecological Regions of the Northwest Territories – Cordillera. Department of Environment and Natural Resources, Government of the Northwest Territories, Yellowknife, NT, Canada. x + 245 pp. + insert map.
- EBA Engineering Consultants Ltd. (EBA). 2001a. Proposed Improvements to Tailing Pond 3, Cantung Mine. Report submitted to North American Tungsten Corporation, June 2001. EBA File No.: 0701-01-14862
- EBA. 2001b. Cantung Mine Abandonment and Restoration Plan, Report submitted to North American Tungsten Corporation Ltd., November 2001. EBA File No.: 701-01-14862.
- EBA. 2001c. Construction Report, Tailings Pond 3 Raise, Cantung Mine, Tungsten, NWT. Report submitted to North American Tungsten Corporation, November 2001. EBA File No.: 0701-01-14862.001
- EBA. 2006. Design Report, Tailings Pond #5 Dam, Cantung Mine, Tungsten, NT. Report submitted to North American Tungsten Ltd., February 2006. File No.: 1200185.
- EBA. 2007a. Design Report for a Raise of the Containment Berm for Tailings Pond 4. Cantung Mine, Tungsten, NT. Prepared for North American Tungsten Corporation Ltd., Vancouver, BC. October 2007. Project Number 704-W14101050.003.
- EBA. 2007b. Cantung Mine Tailings Pond 4 and Tailings Pond 5. Report submitted to North American Tungsten Corporation Ltd., February 5, 2007. File No.: 1200185.002.
- EBA. 2007c. Geophysical Site Investigation, Magnetic Gradient Survey, Tailings Pond 4, Cantung Mine, NT. Report submitted to North American Tungsten Corporation Ltd., October 2007. File No.: W1410105.006.
- EBA. 2007d. Tailings Management Plan for the Cantung Mine, Northwest Territories. Report submitted to North American Tungsten Corporation Ltd., April 2007. File No: 1200185.002.

- EBA. 2008a. Data Report on the Geotechnical Instrumentation of Tailings Pond 4. Cantung Mine, NT. Prepared for North American Tungsten Corporation Ltd., Vancouver, BC. January 2008. Project Number 704-W14101050.007.
- EBA. 2008b. Interim Construction Record Report, Stage 1 Tailings Pond 4 Containment Berm Raise to 3,715 Feet, Cantung Mine, Tungsten NT. Report submitted to North American Tungsten Corporation, January 2008. File No.: W14101050.003.
- EBA. 2008c. Materials Construction Record Report, Stage 2 Tailings Pond 4 Containment Berm Raise to 3,730 Feet, Tungsten NT. Report submitted to North American Tungsten Corporation, January 2008. File No.: W14101050.011.
- EBA. 2009a. 2009 Groundwater Monitoring Well Installations. Cantung Mine, NT. Prepared for North American Tungsten Corporation Ltd., Vancouver, BC. October 2009. Project Number 704-E14101068.014.
- EBA. 2009b. Cantung Mine Abandonment and Reclamation Plan. Report submitted to North American Tungsten Corporation Ltd., Mach 2009. EBA File No.: 1740117.004.
- EBA. 2009c. 2009 Tailings Monitoring Plan, Cantung Mine, NT. Report submitted to North American Tungsten Corporation Ltd., July 2009. File No.: E14101068.018.
- EBA Engineering Consultants Ltd. operating as EBA, A Tetra Tech Company. (EBA, A Tetra Tech Company). 2011. Conversion Between Coordinate Systems, Cantung Mine Site. Technical Memo presented to NATCL, August 3, 2011. EBA File No.: E14101068.023.
- EBA, A Tetra Tech Company. 2012a. Data Report on the Geotechnical Investigation and Groundwater Monitoring Well Installations at Tailings Ponds 1 and 2. Cantung Mine, NT. Prepared for North American Tungsten Corporation Ltd., Vancouver, BC. March 2012. Project Number 704-W23101478.
- EBA, A Tetra Tech Company. 2012b. Cantung 2012 EP1 and TP5 Geotechnical Investigation Summary. Cantung Mine, NT. Prepared for North American Tungsten Corporation Ltd., Vancouver, BC. November 2012. Project Number 704-V15101062.001.
- EBA, A Tetra Tech Company. 2013. Tailings Storage Facility 5, Containment Berm Raise, Cantung Mine, NT. Report submitted to NATCL, January 9, 2013. EBA File No.: V15101062.100.
- Electric Power Research Institute (EPRI). 1993. Guidelines for Site Specific Ground Motions. EPRI TR-102293. Palo Alto, California. November 1993.
- Environment Canada. 2009. Environmental Code of Practice for Metal Mines (PDF copy).
- Golder Associates Ltd. (Golder). 1974. Report to Canada Tungsten Mining Corp. Ltd. On tailings Retention Facilities, Tungsten, N.W.T., July 1974. File No.: V74115
- Golder. 1976a. Future Tailings Disposal. Tungsten, N.W.T. Prepared for Canada Tungsten Mining Corporation Ltd., Vancouver, BC. December 1976.
- Golder. 1976b. Tailings Disposal Ponds Nos. 1 and 2. Tungsten, N.W.T. Prepared for Canada Tungsten Mining Corporation Ltd., Vancouver, BC. May 1976.
- Golder. 1976c. Report to Canada Tungsten Mining Corp. Ltd. On Tailings Disposal Pond 3, Tungsten, N.W.T., May 1976. File No.: 76056-A.
- Golder. 1977a. Hydrology of Tailing Ponds. Tungsten, N.W.T. Prepared for Canada Tungsten Mining Corporation Ltd., Vancouver, BC. January 1977.
- Golder. 1977b. Report to Canada Tungsten Mining Corporation Limited on Possible Long-Term Future Tailings Disposal, March 1977. File No.: V76056-D.
- Golder. 1980. Report to Canada Tungsten Mining Corporation Limited on Development of Tailing Pond No. 3, Tungsten, NWT, July 1980. File No.: 802-1154.
- Golder. 1983. Hydrogeological Investigation – Summer, 1982. Canada Tungsten Mining Site. Tungsten, N.W.T. Prepared for Canada Tungsten Mining Corporation Ltd., Vancouver, BC. January 1983.

- Golder. 1984. Site Visit – September 19 to 21, 1984. Letter submitted to Canada Tungsten Mining Corporation Ltd., November 8, 1984. File No.: E/84/1428.
- Golder. 1985a. Report to Canada Tungsten Mining Corporation on Tailing Disposal at Pond Nos. 3 and 5. January, 1985. File No.: 842-1575.
- Golder. 1985b. Tailings Dam Construction 1985 Season Planning and Method, February 21, 1985.
- Golder. 1985c. Tailings Pond No. 3. Letter to Canada Tungsten Mining Corporation, June 3, 1985. File No.: E/85/544.
- Golder. 1985d. Assessment of Tailings Pond #3 Storage Capacity. Letter to Canada Tungsten Mining Corporation Limited, December 12, 1985.
- Grozic, J.L.H., Imam, S.M.R., Robertson, P.K., and Morgenstern, N.R. 2005. Constitutive modeling of gassy sand behaviour. Canadian Geotechnical Journal. 812-829.
- Harder, L.F, and Seed, H.B. 1986. Determination of Penetration Resistance of Coarse Grained Soils using the Becker Hammer Drill. Report No. UCB/EERC-86/06. Earthquake Engineering Centre, University of California, Berkeley.
- Idriss, I. M., and Boulanger, R. W. 2008. Soil liquefaction during earthquakes. Monograph MNO-12, Earthquake Engineering Research Institute, Oakland, CA, 261 pp.
- Ishihara, K., Tsuchiya, H., Kamada, K. 2001. Recent Studies on Liquefaction Resistance of Sand - Effect of Saturation. International Conferences on Recent Advances in Geotechnical Earthquake Engineering and Soil Dynamics. Keynote Lecture.
- Itasca (2016). FLAC: Fast Lagrangian Analysis of Continua. Version 8.0. Minneapolis, Minnesota, USA.
- Knight Piesold Consulting Ltd. (Knight Piesold). 2011. TSF 4 Stage 4 and TSF5 Stage 1-B Construction Report. Report submitted to North American Tungsten Corporation Ltd., December 2011. File No.: VA101-433/9-2.
- Knight Piesold. 2011. Knight Piesold Consulting, 2011. TSF 4 Stage 4 and TSF5 Stage 1-B Construction Report. Report submitted to North American Tungsten Corporation Ltd., December 2011. File No.: VA101-433/9-2.
- Knight Piesold. 2012a. Stability Assessment for Tailings Storage Facility 4. Cantung Mine Project. Prepared for North American Tungsten Corporation Ltd., Vancouver, BC. January 2012.
- Knight Piesold. 2012b. 2012 Tailings Management Plan. Report submitted to North American Tungsten Corporation Ltd., January 2012. File No.: VA101-433/10-1.
- Kulhawy, F.H., and Mayne, P.H., 1990. Manual on estimating soil properties for foundation design. Report EL-6800 Electric Power Research Institute, EPRI, August 1990.
- Mackenzie Valley Land and Water Board (MVLWB) and Aboriginal and Northern Development Canada (AANDC), 2013. Guidelines for the Closure and Reclamation of Advanced Mineral Exploration and Mine Sites in the Northwest Territories, November 2013.
- Mayne, P.W., Christopher, B.R., and DeJong, J. 2001. Manual on Subsurface Investigations. National Highway Institute Publication No. FHWA NHI-01-031, Federal Highway Administration, Washington, DC, July 2001.
- Mining Associated of Canada (MAC). 2019. A Guide to the Management of Tailings Facilities, Version 3.1. February 2019. Accessed from <https://mining.ca/documents/a-guide-to-the-management-of-tailings-facilities-version-3-1-2019/>, August 8, 2020.
- Montgomery, J. and Boulanger, R.W. 2016. Effects of Spatial Variability on Liquefaction-Induced Settlement and Lateral Spreading. Journal of Geotechnical and Geoenvironmental Engineering, ASCE, 04016086, 10.1061/(ASCE)GT.1943-5606.0001584.
- North American Tungsten Corporation Ltd (NATCL). 1986. Tailings Storage and Backfill. Memo to E. Ladner/J.Wilson from R. Allan, July 29, 1986. File No. 5.10.3.

- NATCL. 2014. Hazardous Waste Management Plan. Cantung Mine, NT. Internal report by North American Tungsten Corporation Ltd. January 2014.
- NATCL. 2015. 2015 Interim Closure and Reclamation Plan, Cantung Mine, NT. Draft 1 – Issued for Review. Prepared for Mackenzie Valley Land and Water Board, Yellowknife, NT. April 2015.
- National Research Council (NRC). 2015. National Building Code of Canada 2015 [NBCC 2015]. 14th Ed. Ottawa, Ontario: National Research Council of Canada.
- National Resources Canada (NRCan). Aerial Photos. A12270 (1949), A12278 (1949), A12637 (1950), A171105 (1960), A20849 (1968), A22355 (1971), A24528 (1976), A26158 (1982)
- NRC. 2010. National Building Code of Canada 2010 [NBCC 2010]. 13th Ed. Ottawa, Ontario: National Research Council of Canada.
- Onur Seeman Consulting Inc. (OSC). 2019. Seismic Hazard and Ground Motions for Cantung Project. Revision 4. Prepared for Tetra Tech Canada Inc., Vancouver, BC. April 2019.
- Ordonez, G. 2011. SHAKE2000: A Computer Program for the 1D Analysis of Geotechnical Earthquake Engineering Problems.
- Robertson, P.K., and Cabal, K.L. 2010. Estimating soil unit weight from CPT. Proceedings of the 2nd International Symposium on Cone Penetration Testing, Huntington Beach, CA, USA, May 2010.
- Rollins, K.M., Evans, M.D., Diehl, N.B. and Daily, W.D. III. 1998. Shear Modulus and Damping Relationships for Gravels. ASCE Journal of Geotechnical and Geoenvironmental Engineering, Vol. 124, (5):396-405.
- Schmertmann, J.H. (1975). Measurement of in-situ shear strength. Proceedings of In-Situ Measurement of Soil Properties, Vol. 2, ASCE, New York, 57-138.
- Seed, H.B. and Idriss, I.M. 1970. Soil Moduli and Damping Factors for Dynamic Response Analysis. Report No. EERC 70-10, University of California, Berkeley, December 1970.
- Stantec, 2014. Cantung Mine, Northwest Territories – Preliminary Terrain Mapping. Memorandum presented to North American Tungsten Ltd., November 26, 2014. File No.: 123311654.
- Sy, A. and Campanella, RG. 1993. BPT-SPT Correlation with Consideration of Casing Friction. 6th Canadian Geotechnical Conference, Saskatoon, Saskatchewan, Sept. 27-29.
- SRK Consulting (Canada) Inc. (SRK). 2012. Cantung Mine – 2017 Dam Safety Review. Prepared for North American Tungsten Corporation Ltd., Vancouver, BC. November 2012.
- SRK. 2015. Assessment of Liquefaction Potential, Dam Stability and Remedial Options at TP 4. Cantung Mine, NT. Prepared for North American Tungsten Corporation Ltd., Vancouver, BC. July 2015.
- SRK. 2017a. Assessment of Liquefaction Potential, Dam Stability and Remedial Options for the Tailings Facilities. Cantung Mine, NT. Prepared for North American Tungsten Corporation Ltd., Vancouver, BC. July 2017.
- SRK. 2017b. 2017 Dam Safety Review for the Tailings Storage Facility, Cantung Tungsten Mine, Northwest Territories. Prepared for North American Tungsten Corporation Ltd., Vancouver, BC. December 2017.
- Tetra Tech Canada Inc. (Tetra Tech) 2019a. 2019 Geotechnical Investigation Data Report, Cantung Mine, NT. Prepared for North American Tungsten Corporation Ltd. c/o Alvarez & Marsal Canada Inc., Vancouver, BC. November 2019 (Issued for Review). Project Number 704-ENW.WENW03039-04.
- Tetra Tech, 2019b. 2019 Annual Inspection – Tailings Storage Facilities, Cantung Mine, Tungsten, NT Report submitted to NATCL, November, 2019. Tetra Tech File No.: 704-ENW.WARC03730-01.
- Tetra Tech. 2020a. Phase III Environmental Site Assessment. Cantung Mine, NT (IFR). Prepared for North American Tungsten Corporation Ltd. c/o Alvarez & Marsal Canada Inc., Vancouver, BC. June 2020. Project Number 704-ENW.WENW03039-03.

- Tetra Tech. 2020b. Conceptual Site Model, Cantung Mine, NT (IFR). Prepared for North American Tungsten Corporation Ltd. c/o Alvarez & Marsal Canada Inc., Vancouver, BC. July 2020. Project No.: 704-ENW.WENW03039-03.004.
- Tetra Tech. 2020c. Terrain and Borrow Source Assessment, Cantung Mine NWT. Prepared for North American Tungsten Corporation Ltd. c/o Alvarez & Marsal Canada Inc., Vancouver, BC. May 2020. Project No.: 704-ENW.WENW03039-04.
- Tetra Tech EBA Inc. (Tetra Tech EBA). 2015. Tailings Pond 5, Stage 3 Dam Raise: Construction Record Report. Prepared for North American Tungsten Corporation Ltd. October 2015. Project Number V15101062.106.
- Tetra Tech EBA, 2014a. Preliminary Design Report. Cantung TSF4b Dry Stack Tailings Storage Facility, Tungsten, NT. Prepared for North American Tungsten Corporation Ltd., Vancouver, BC. February 2014. Project Number V15101062.150.
- Tetra Tech EBA. 2014b. Preliminary Design Report. TSF6 Dry Stack Tailings Storage Facility, Cantung Mine, Tungsten, NT. Prepared for North American Tungsten Corporation Ltd., Vancouver, BC. March 2014. Project Number V15101062.204.
- Tetra Tech EBA. 2014c. Cantung TSF7 Dry Stack Tailings Storage Facility. Preliminary Design Report. Prepared for North American Tungsten Corporation Ltd., Vancouver, BC. March 2014. Project Number V15101062.250.
- Tokimatsu, A.M. and Seed, H.B. (1987). Evaluation of settlements in sands due to earthquake shaking. Journal of Geotechnical Engineering 113 (11), ASCE.
- Wu, J. (2002). Liquefaction triggering and post liquefaction deformations of Monterey 0/30 sand under uni-directional cyclic simple shear loading. PHD Dissertation, University of California, Berkeley.